AD-A111 681   LOCKHEED MISSILES AND SPACE CO INC PALO ALTO CA PALO --ETC   F/G 12/1
IMPERFECTION SENSITIVITY OF OPTIMIZED STRUCTURES.(U)
MAR 81   B O ALMROTH, P STERN, D BUSHNELL   F33615-76-C-3105
UNCLASSIFIED   AFWAL-TR-80-3128   NL

END
DATE
FILMED
4-82
DTIC

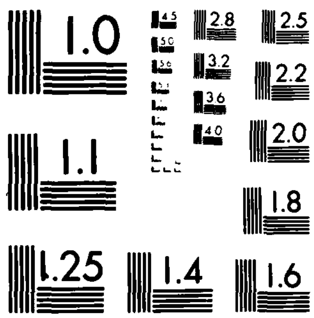
1.0
1.1
1.25
1.4
1.6
1.8
2.0
2.2
2.5
2.8
3.2
3.6
4.0

AFWAL-TR-80-3128

IMPERFECTION SENSITIVITY OF OPTIMIZED STRUCTURES

B. O. ALMROTH
P. STERN
D. BUSHNELL

LOCKHEED MISSILES AND SPACE COMPANY, INC.
3251 HANOVER STREET
PALO ALTO, CALIFORNIA 94304

MARCH 1981

TECHNICAL REPORT AFWAL-80-3128
Final Report for Period June 1976 - October 1980

FLIGHT DYNAMICS LABORATORY
AIR FORCE WRIGHT AERONAUTICAL LABORATORIES
AIR FORCE SYSTEMS COMMAND
WRIGHT-PATTERSON AIR FORCE BASE, OHIO 45433

NOTICE

When Government drawings, specifications, or other data are used for any purpose other than in connection with a definitely related Government procurement operation, the United States Government thereby incurs no responsibility nor any obligation whatsoever; and the fact that the government may have formulated, furnished, or in any way supplied the said drawings, specifications, or other data, is not to be regarded by implication or otherwise as in any manner licensing the holder or any other person or corporation, or conveying any rights or permission to manufacture use, or sell any patented invention that may in any way be related thereto.

This report has been reviewed by the Office of Public Affairs (ASD/PA) and is releasable to the National Technical Information Service (NTIS). At NTIS, it will be available to the general public, including foreign nations.

This technical report has been reviewed and is approved for publication.

Narendra S. Khot

NARENDRA S. KHOT,
Project Engineer

Fred A. Picchioni

FREDERICK A. PICCHIONI, Lt Col, USAF
Chief, Analysis & Optimization Branch

FOR THE COMMANDER

Ralph L. Kuster

RALPH L. KUSTER, JR., Col, USAF
Chief, Structures & Dynamics Div.

"If your address has changed, if you wish to be removed from our mailing list, or if the addressee is no longer employed by your organization please notify AFWAL/FIBR, W-PAFB, OH 45433 to help us maintain a current mailing list".

Copies of this report should not be returned unless return is required by security considerations, contractual obligations, or notice on a specific document.

UNCLASSIFIED

SECURITY CLASSIFICATION OF THIS PAGE (When Data Entered)

REPORT DOCUMENTATION PAGE

READ INSTRUCTIONS BEFORE COMPLETING FORM

1. REPORT NUMBER: AFWAL-TR-80-3128	2. GOVT ACCESSION NO.
3. RECIPIENT'S CATALOG NUMBER	
4. TITLE (and Subtitle): Imperfection Sensitivity of Optimized Structures	5. TYPE OF REPORT & PERIOD COVERED: Final Report for Period June 1976-Oct. 1980
	6. PERFORMING ORG. REPORT NUMBER
7. AUTHOR(s): B. O. Almroth, P. Stern, D. Bushnell	8. CONTRACT OR GRANT NUMBER(s): F33615-76-C-3105
9. PERFORMING ORGANIZATION NAME AND ADDRESS: Lockheed Missiles and Space Company, Inc. 3251 Hanover Street Palo Alto, California 94304	10. PROGRAM ELEMENT, PROJECT, TASK AREA & WORK UNIT NUMBERS: 2307-N1-02
11. CONTROLLING OFFICE NAME AND ADDRESS: AFWAL/FIBRA, U.S. Air Force, Aeronautical Systems Division, Wright Patterson Air Force Base, Ohio	12. REPORT DATE: March 1981
	13. NUMBER OF PAGES: 55
14. MONITORING AGENCY NAME & ADDRESS (if different from Controlling Office)	15. SECURITY CLASS. (of this report): Unclassified
	15a. DECLASSIFICATION/DOWNGRADING SCHEDULE

16. DISTRIBUTION STATEMENT (of this Report)

Approved for public release; distribution Unlimited

17. DISTRIBUTION STATEMENT (of the abstract entered in Block 20, if different from Report)

18. SUPPLEMENTARY NOTES

19. KEY WORDS (Continue on reverse side if necessary and identify by block number)

Structural Panels, Composite Materials, Stability, Im[illegible]tion Sensitivity

20. ABSTRACT (Continue on reverse side if necessary and identify by block number)

There is a tendency of the critical load to become unstable if the lowest buckling modes are simultaneous or nearly so. This tends to be the case if structural panels are optimized with bifurcation buckling constraints.

A complete software package, POIS (Panel Optimization with Integrated Software), was developed to solve this problem. POIS is described in a separate report with a summary presented here. The pre-buckling nonlinear behavior due to geometric imperfections is taken into account.

DD FORM 1 JAN 73 1473 EDITION OF 1 NOV 65 IS OBSOLETE

UNCLASSIFIED

SECURITY CLASSIFICATION OF THIS PAGE (When Data Entered)

20. - CONTINUED

The procedure allows optimization with the collapse load as constraint for panels that buckle locally well below the ultimate load. The computer programs are verified by application in some practical cases involving metal and composite material panels. It is concluded that the most weight - efficient design is one in which local buckling is permitted. A supplementary experimental program should be executed before POIS can be qualified as a reliable instrument for panel design.

FOREWORD

This report was prepared by Lockheed Missiles and Space Company, Inc., Palo Alto Research Laboratories, 3251 Hanover Street, Palo Alto, California, in partial fulfillment of the requirements under Contract F33615-76-C-3105. The effort was initiated by Dr. L. Berke under Project 2307, "Research in Flight Vehicle Structures," Task 2307N102, "Research in the Behavior of Metallic and Composite Components of Air Frame Structures." The project monitor for the contract was Dr. Narendra S. Khot of the Structures and Dynamics Division (AFWAL/FIBRA).

The technical work under the contract was performed during the period June 1976 through October 1980. Review report was submitted in October 1980 and the final report in March 1981.

The other reports published under this contract are "Numerical Procedure for Analysis of Structural Shells," (AFWAL-TR-80-3129), "Panel Optimization with Integrated Software (POIS)," (AFWAL-TR-80-3073, Vol I and II), "Design of Composite Material Structures for Buckling, An Evaluation of State-of-the-Art," (AFWAL-TR-81-3102), "Supplementary Studies on the Sensitivity of Optimized Structures," (AFWAL-TR-81-3013).

TABLE OF CONTENTS

LIST OF ILLUSTRATIONS

LIST OF ILLUSTRATIONS (Cont.)

LIST OF TABLES

Section I
SUMMARY

It has long been known that buckling loads tend to become sensitive to geometric imperfections whenever the lowest buckling loads are simultaneous or nearly simultaneous. That is, if two or more eigenvalues are closely clustered, interaction between these modes may cause imperfection sensitivity.

Optimization with stability constraints is severely complicated by such imperfection sensitivity. During optimization the critical load must be computed a large number of times. The critical load is obtained after a set of imperfection patterns are selected at random and a nonlinear analysis is performed with each of these, so that, for example the load level corresponding to a 99 percent probability of success can be determined. In the optimization procedure presented here the number of nonlinear analyses is reduced by use of a three staged approach. In this approach the structural panels are first optimized with bifurcation buckling constraints. This optimization is performed at a sequence of load levels spanning the range of loads for which panel designs are required. Computer economy allows us to leave one decision parameter to be determined in the final phase, i.e., the nonlinear analysis. Previous experience indicates that the parameter that has the most severe impact on the knockdown factor is the ratio between the local and general instability limits. Therefore this parameter is left to be determined in the final nonlinear analysis.

Computer software for optimization of stiffened structural panels with due consideration to possible imperfection sensitivity has been developed under the present contract. The software is referred to by the code name POIS (Panel Optimization with Integrated Software). In POIS panels may be optimized in three stages. In the first two stages, PANDA and ECHO, the panels are assumed to be perfect. In the first stage an interactive program (PANDA) is used to determine initial values for the design parameters. These initial values are determined at a number of load levels for each of a sequence of values of the local/general buckling ratio. The equations for local and general instability eigenvalues are derived in PANDA with the use of simple assumed trigonometric and power law expressions for the buckling modal displacements. In the second

stage (ECHO), a processor called FRITZ (for "Fast-Ritz") computes bifurcation buckling loads based on modes defined by the program user in terms of trigonometric series. ECHO applies to panels with other than simply supported edges, to which PANDA is restricted. Depending on the user's choice of Ritz functions, more accurate buckling loads may be determined than is possible with PANDA. ECHO is also more general than PANDA with regard to loading. The computer time required for running ECHO is somewhat more than that required for running PANDA. In addition to FRITZ, the programs STAGSC-1 and VIPASA also reside in ECHO. However, these are used mainly for verification of the buckling analysis based on the FRITZ program.

For relatively simple panels (flat or cylindrical with rectangular planform), nonlinear collapse analysis can also be performed in ECHO. The user defines deformation modes and solutions are sought in a reduced space of displacements configurations defined by all linear combinations of these modes. A STAGS finite element model is used only for numerical integration to define the coefficients of the reduced system. Failure criteria are built into the program to test whether local values of the strain exceed their upper limits before a point of maximum load in a load displacement diagram is reached.

For more complex panel configurations the final nonlinear phase of the analysis can be performed in RRSYS, a program complex developed under contract with NASA Langley and modified under the present contract for the purpose of panel optimization. In RRSYS the nonlinear analysis can be carried out in FRITZ, which resides in RRSYS as well as in ECHO, or in a Rayleigh-Ritz analysis used in conjunction with a finite element model. The latter procedure expands the set of panel geometries that can be handled with POIS.

For demonstration of the POIS system, five different (metal and composite) panels were optimized. The nonlinear analysis was carried out only in one case. The success of optimization with POIS clearly depends on a capability to define the parameters governing the random imperfections. As a consequence it is felt that any further progress in this area will be possible only if the effort is augmented with a carefully executed experimental program.

SECTION II

INTRODUCTION

It has long been known that the buckling load tends to become sensitive to geometric imperfections whenever the lowest buckling modes are simultaneous or nearly simultaneous. That is, if two or more eigenvalues are closely clustered, interaction between corresponding modes may cause imperfection sensitivity. It was pointed out in 1962 by Koiter and Skaloud (Reference 1) that this sensitivity may nullify optimum weight criteria and thus refer to these as the "naive" approach to optimization.

Experimental evidence of imperfection sensitivity due to interaction between local and general instability modes was available in 1934 (Reference 2). Later Thompson et al (Reference 3) produced and tested integrally stiffened wide plates with systematically varied imperfections. Van der Neut in 1969 (Reference 4) presented the first paper in which the imperfection sensitivity was established by analytical means. Tvergaard (Reference 5) investigated the stability and imperfection sensitivity of the integrally stiffened wide plate as a two-degree-of-freedom system. The general instability (wide column) buckling mode and the lowest local skin buckling mode are the only deformation modes included in that analysis. The results shown in Figure 1 apply in the case with fixed stiffener spacing. Here h_o is the skin thickness corresponding to an Euler load (wide column buckling) of λ_o in the absence of any stiffening. That is, at $h/h_o=1$ the Euler column load corresponds to $\lambda/\lambda_o=1$. The efficiency of the design is improved if some material is removed from the skin and used in stiffeners. The graph depicts the situation in which the skin thickness h is varied in such a way that the total weight, stiffener plus skin, is constant. The curves correspond to the case in which $a/b=4$, $e/b=0.05$ and $h_o/b=0.0128$ where b is the panel length, a is the stiffener spacing and e the stiffener eccentricity. The amplitude w_i of the imperfection applies to the local as well as to the general mode.

With constant stiffener spacing the local buckling load decreases with decreasing skin thickness h, such that at $h/h_o=0$ local buckling corresponds to $\lambda/\lambda_o=0$. With decreasing h the Euler load obviously increases due to the increase in cross-section moment of inertia as the stiffness increases in height. The point where the two

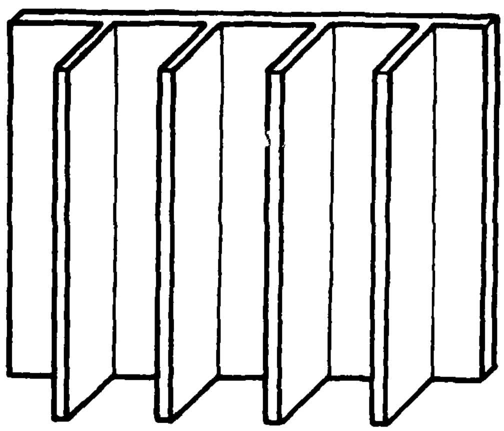

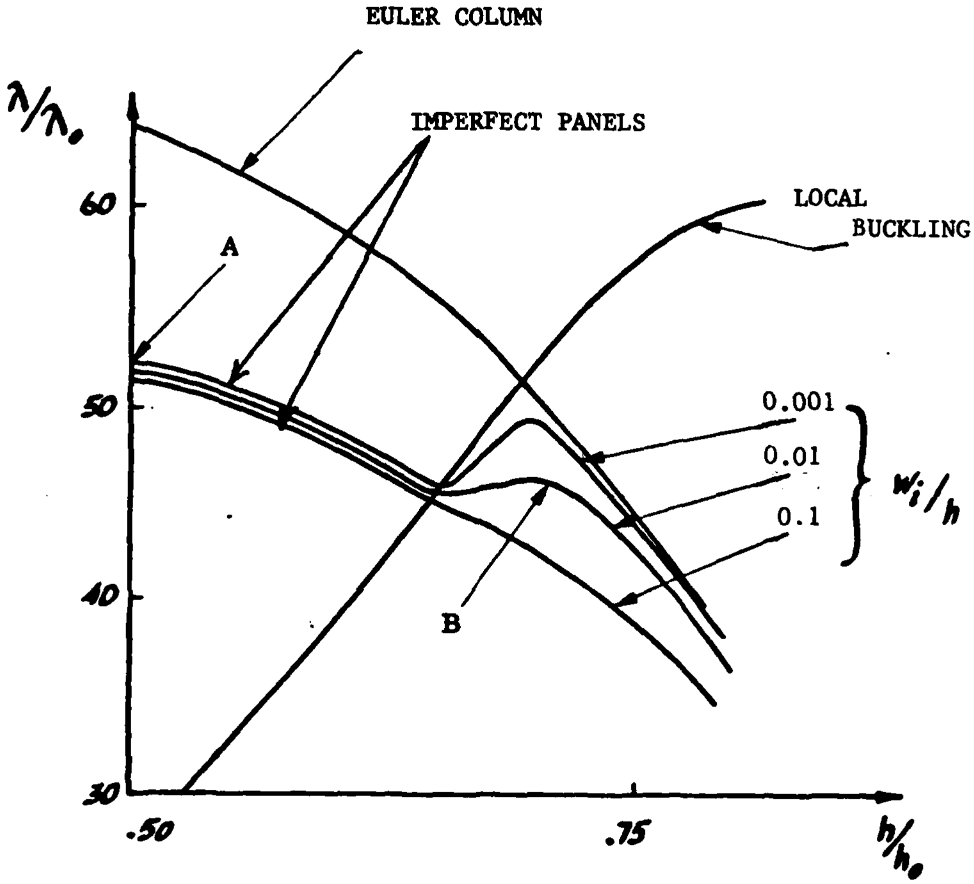

Figure 1 Imperfection Sensitivity of Stiffened Wide Plate

curves intersect is the optimum design according to the simultaneous mode criterion. For bifurcation buckling of a perfect structure it is also a true optimum, except for the fact that the wide column analysis with smeared stiffeners neglects the effect of cross-section deformation and warping. In reality shear lag effects and local transverse bending will prevent the skin from full participation in the resistance to overall panel bending.

Tvergaard's curves for imperfect panels correspond to collapse at a limit point rather than a bifurcation buckling load. For very small imperfections the curves in Figure 1 have local maxima close to the bifurcation point for the optimized perfect panel. However, the curves also show that we can reach higher values of the load without collapse, but with a deeply wrinkled skin. For example, with $w_i/h=0.01$ the collapse load at A ($h/h_o = 0.48$) is 12 percent higher than it is for the "optimum structure" at B and it is almost twice the load at which local buckles initiate in the skin between the stiffeners.

It is clear from the curves in Figure 1 that the knock-down factor, if we consider the collapse load as the critical load, varies with the geometric parameters. The knock-down factor varies with h/h_o or equivalently with the ratio ϕ between local and general bifurcation buckling loads. Thus, we cannot determine a value of the knock-down factor in advance. To obtain a critical load it is necessary to generate a set of random imperfection patterns and to perform a nonlinear analysis corresponding to each of these, so that the load level corresponding to a one percent probability (or some other probability) of collapse can be determined.

In addition to the neglect of shear lag effects the analysis by Tvergaard includes other approximations. The deterioration of the stiffener's resistance to rotation about its axis of attachment to the skin with increasing load is not included. Only one local mode is considered. Further, the behavior of a wide, flat plate does not necessarily reveal much about the cases of slightly curved plates with simply supported longitudinal edges, which are more interesting to designers of airplanes. A flat plate with supported edges will probably exhibit stable equilibrium in the early postbuckling range, since the support along the edges allows redistribution of stresses. The imperfection sensitivity and modal interaction manifests itself then in the form of rapidly growing local deformation. This deformation may lead to fracture in composite materials or unacceptable

permanent deformation in metals. On the other hand a curved panel may collapse at an imperfection sensitive limit point even if the lower eigenvalues are well separated. In view of such problems Budiansky and Hutchinson (Reference 6) suggest that the "subject of mode interaction in practical structures may be ripe for brutal computerization".

Computer software for optimization of stiffened structural panels with due consideration to possible imperfection sensitivity has been developed under the present contract. The software is referred to by the code name POIS (Panel Optimization with Integrated Software). This report discusses first, as a background the basic concept of structural stability and the practical consequences of loss of stability. Thereafter follows a general discussion of the approach to optimization of imperfection sensitive structures, a brief description of POIS, and finally a presentation of some numerical results obtained for its verification. Some conclusions are made about the need to consider the problem of mode interaction in the design of structural panels typical of airplane designs.

Section III

THE CONCEPT OF STABILITY

The wor l buckling conveys a visual conception of the structural deformation but does not have a rigorous scientific or mathematical definition. On the other hand the phrases "bifurcation buckling" and "limit point" refer to a loss of structural stability and can be defined in mathematical terms. However, the designer's interest is in the load limit below which deformations and stresses are of acceptable magnitudes. This limit does not necessarily coincide with the limit of structural stability. However, the concept of stability is still useful in determining the behavior of structures that exhibit geometrically nonlinear behavior.

The definition of stable equilibrium of a deformable body follows as an obvious extension of the concept of stable equilibrium of a rigid body. A given displacement field u corresponds to stable equilibrium if the imposition of any additional permissible (by continuity and boundary conditions) displacement field perturbation Δu of sufficiently small amplitude generates

forces that tend to restore the basic displacement field u. This is equivalent to the requirement that the displacement field u corresponds to a true minimum of the total potential energy. The body is in unstable equilibrium if the potential energy has a maximum or an inflexion with zero slope with respect to at least one of its degrees of freedom. A couple of simple examples will be considered for clarification of the concept and establishment of some definitions.

The load displacement relation representing static equilibrium for a shallow link system is indicated in Figure 2. The equilibrium is stable on the parts of the curve at which the load increases with the deformation, and it is unstable (as indicated by a dotted line) in the range where the curve has a negative slope. If the load is increased beyond the <u>limit point</u> at A, there is no equilibrium configuration available in the immediate neighborhood. Therefore, the structure must be set in motion. In this particular case, the link system "<u>snaps through</u>" into a configuration at point B with tension forces in the links. The transition is a dynamic phenomenon.

For sufficiently small loads, a centrally loaded column exhibits no rotation in its deformation pattern. In the range of small strain, its behavior is linear. A path in the load displacement diagram that passes through the origin is referred to as the <u>primary path</u>. The path depicting the maximum lateral displacement versus axial load coincides with the vertical axis (Figure 3). Due to the nonlinear character of the governing equations, secondary solutions corresponding to bent equilibrium forms also exist, although not in the immediate neighborhood of the origin. Whether or not the primary path is linear, there is a possibility that it is intersected by a path corresponding to a secondary solution as indicated in Figure 3. The point of intersection between the two load paths is referred to as a <u>bifurcation point</u> and the corresponding load is called the bifurcation buckling load. It is the smallest load at which a bent column can represent an equilibrium configuration.

Bifurcation points can be found by use of a linearized analysis. The equations that govern the structural behavior are of the form

$$L(u) = 0 \qquad (1)$$

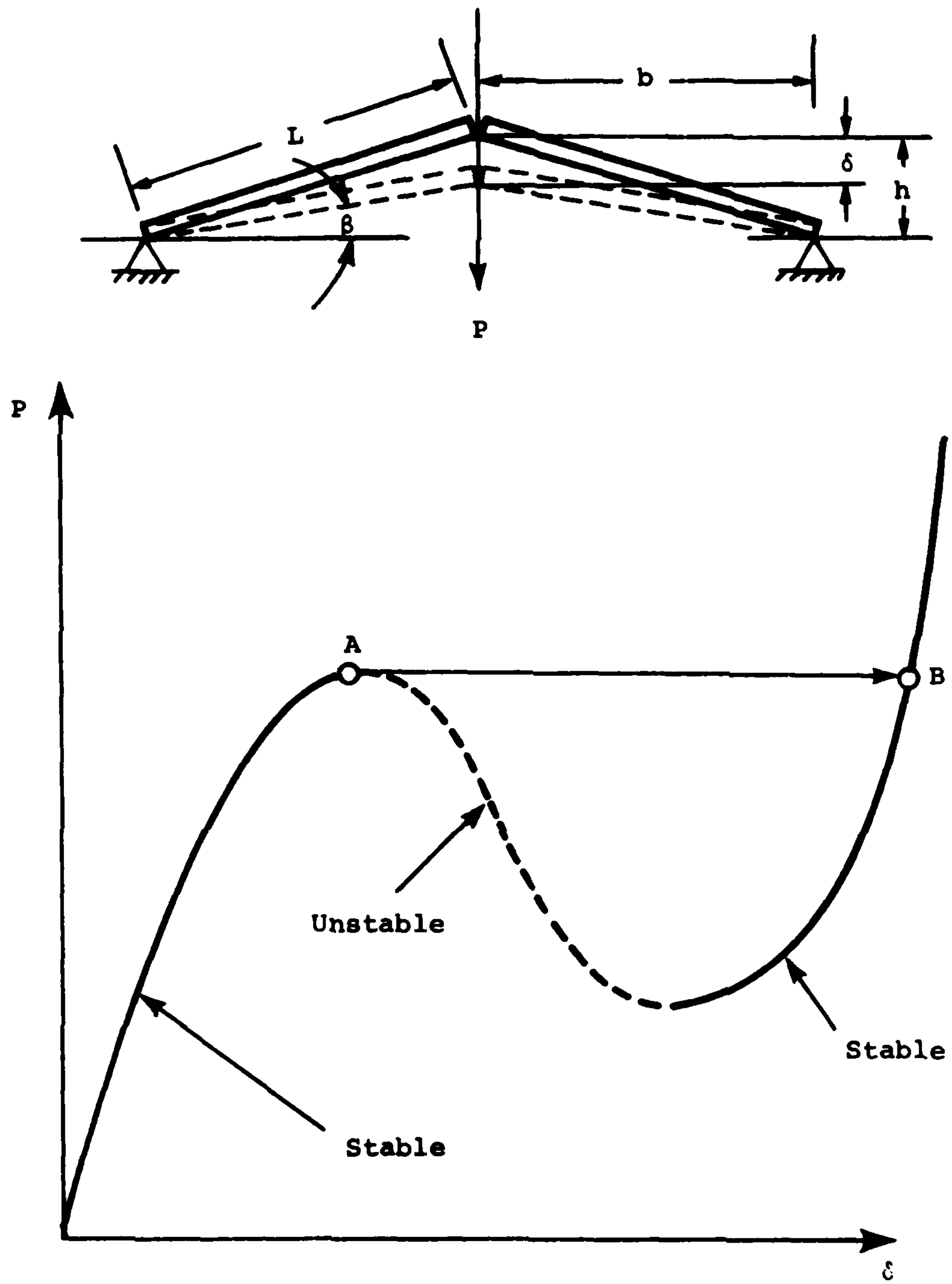

Figure 2 Load Displacement Curve for a Shallow Link System

where L is a nonlinear differential operator. If u_o represents an equilibrium configuration on the primary path, then $L(u_o)=0$. At any point of intersection with a secondary path Equation 1 must have multiple solutions. The existence of multiple solutions can be determined from the equation.

$$L(u_o + \Delta u) - L(u_o) = 0 \tag{2}$$

All terms in this equation that do not contain the incremental displacement Δu cancel one another since $L(u_o) = 0$. If, in addition, Δu is small enough so that higher order terms may be omitted, Equation 2 becomes homogenous. The trivial solution $\Delta u = 0$ corresponds to equilibrium on the primary path. The existence of a nontrivial solution at some load level indicates the presence of a bifurcation point. This value of the load parameter is the eigenvalue and the nontrivial solution for Δu is the eigenfunction or, for a discrete system, the eigenvector. The eigenfunction defines the deformation mode on the secondary path in the immediate neighborhood of the bifurcation point. This deformation pattern, the buckling mode, is distinct from the deformation pattern on the primary path. Bifurcation can occur only into some deformation pattern that is orthogonal to the deformation pattern on the primary path.

The meaning of this orthogonality requirement may be clarified by observation of the behavior of a structure with some degree of imperfection. If, for example, a column has some small initial curvature or some eccentricity in loading, the straight form is not an equilibrium configuration at any load level. There is no bifurcation point, but the primary path for the imperfect column gradually approaches the secondary path for the perfect column as indicated in Figure 3.

It can be shown that the equilibrium on the primary path loses its stability at the first bifurcation point. Consequently, the limit of stability can be determined either through consideration of adjacent equilibrium as discussed above or through a consideration of the total potential energy of the system. The structure will cease to be in stable equilibrium when the load is raised to such a level that the total potential energy is no longer a true minimum. That is, the level at which the second variation of the potential energy ceases to be positive definite.

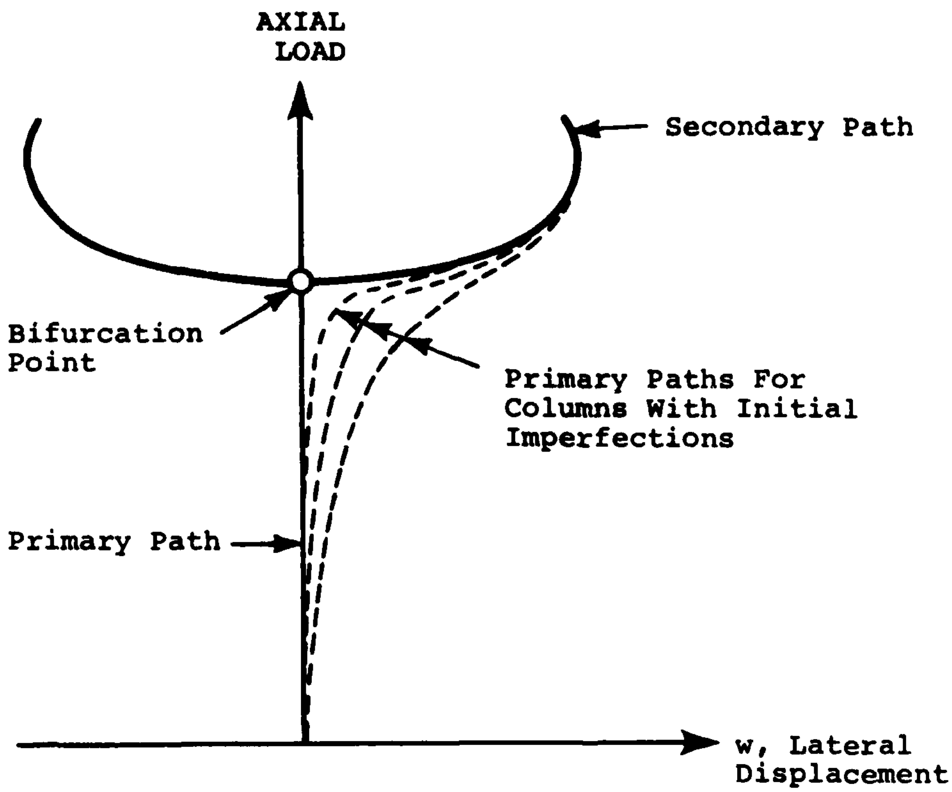

Figure 3 Equilibrium Paths for Column

Section IV
THE CONSEQUENCES OF INSTABILITY

The primary interest of a structural designer is not whether one form of equilibrium or another is stable, but rather how the structure responds to a given loading environment in terms of stresses and deformations. The stability concept is useful only if it is possible to foresee how instability in a given case affects the general structural behavior.

First we consider the case in which stability is lost at a limit point. If the load is controlled, rather than the displacement, the structure will be set in motion when the critical load is exceeded. Exactly how violent the snap-through is and how badly deformed the structure is after it has come to rest in another stable equilibrium configuration can only be determined by use of a postbuckling analysis. A true representation of the structural behavior can be determined if, after static loading to a level just below the limit point, the analysis is restarted in a dynamic mode (including damping) at a load level just above the limit point. However, it is usually assumed that a limit point represents the ultimate load carrying capability of the structure, although it is possible in a complex, redundant structure that the snap-through only occurs in a small and rather insignificant part of the structure.

The effect of bifurcation on the general structural behavior is not immediately clear. As the equilibrium on the primary path loses its stability at the bifurcation point, the structural behavior beyond bifurcation is governed by the conditions on the secondary path. Thus a bifurcation point signifies a load level at which a new deformation pattern begins to develop. The primary path defines the prebuckling behavior and the secondary path the postbuckling behavior. If the equilibrium on the secondary path is stable at the bifurcation point, the structure may have considerable postbuckling strength. The loss of stability of the equilibrium on the primary path need not mean that the structure collapses.

On the other hand, if equilibrium on the secondary path in unstable at the bifurcation point, buckling is sudden and the buckling load of the structure may be sensitive to imperfections. The behavior of the structure is much the same as it is at a limit point. Actually, if a small imperfection in the form of the buckling mode is included, a limit point will occur just below the bifurcation point for the perfect structure. Three different types of behavior at a bifurcation point are illustrated in Figure 4.

The type of behavior indicated in case (a) corresponds to stable equilibrium on the postbuckling branch. In such a case, the occurrence of bifurcation may be of little consequence.

A column under an axial load shows a considerable lateral displacement at load levels only slightly above the bifurcation buckling load. Flat plates with supported edges under shear or compressive loading exhibit substantial post-buckling strength. The plate stiffness is significantly reduced at the bifurcation point but remains substantial. The cases (b) and (c) indicate the structural behavior in case the equilibrium is unstable on the secondary path. The limit point for the imperfect structure may be well below the bifurcation point for the perfect structure.

Detailed information about the structural behavior beyond bifurcation can be obtained if the secondary path is traced through solution of the nonlinear equilibrium equations. However useful, information may be obtained with the Koiter theory, (Reference 7). This theory is based on determination of the stability of equilibrium on the intersecting secondary path at the bifurcation point. Koiter theory determines which of three cases in Figure 4 represents the structural behavior.

Section V

OPTIMIZATION STRATEGY

The appropriate constraint in structural optimization is, of course, the degree of severety of the environment that can be suffered by the structure without unacceptable consequences. The bifurcation buckling load may because of imperfection sensitivity have little meaning as a design parameter, even if

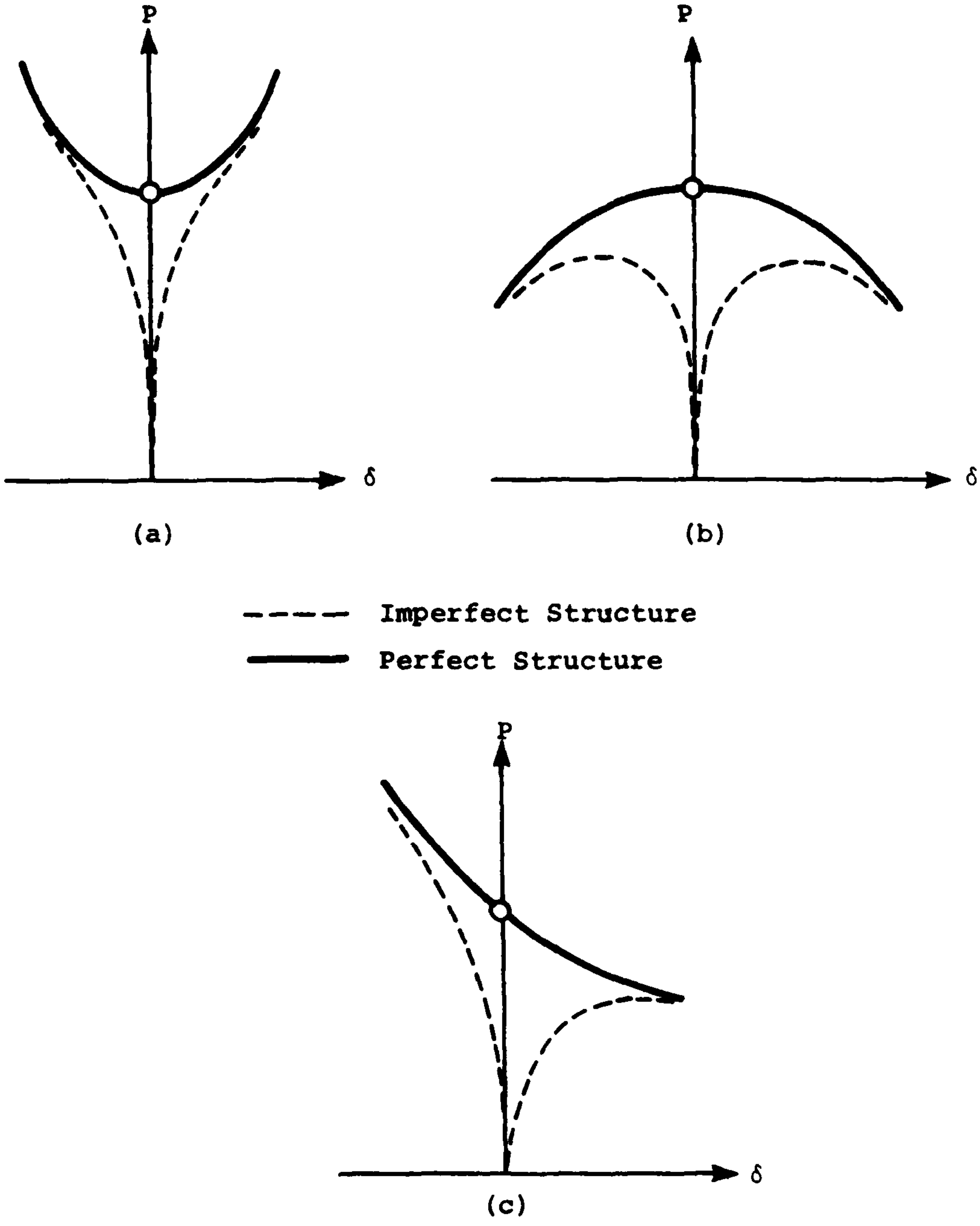

Figure 4 Typical Load-Displacement Relations

the structure is stability critical. When the structure is imperfection sensitive and, as always, some more or less random imperfections are present, the ultimate load is a stochastic variable. It may, for example, be defined as the load level corresponding to a 99 percent probability that the structure will not suffer unacceptable damage.

To establish the value of the ultimate load of an imperfection sensitive structure we must perform a nonlinear analysis a number of times, each one with independently determined imperfections. These are defined by some random procedure with practical constraints on amplitudes and wavelengths. The procedure must be repeated at least ten to twenty times in order to allow subsequent statistical analysis of the results. With a relatively large number of optimization parameters and more than one load case, the constraint function (the ultimate load) must be computed a large number of times, maybe several hundreds. Under such circumstances it is clearly not feasible to determine the constraint function each time by use of the procedure outlined above. The problem is aggravated if optimum dimensions are to be established for a sequence of load levels. The question arises of whether it is possible to determine in advance a ratio between the ultimate load and the bifurcation buckling load. The constraint function will then be given by this *knock-down factor* times the bifurcation buckling load.

In Reference 8 Koiter and Pignataro give an equation for the knock-down factor as a function of two parameters. One is the ratio between the local and general stability limits and the other is a nondimensional geometric parameter. Unfortunately, this equation is applicable only to the blade-stiffened, flat and infinitely wide plate under pure axial compression. It does not seem feasible to derive similar expressions for the great variety of situations that must be covered by an adequate computer program for optimization of airplane wing and fuselage panels. The use of an a priori knock-down factor approach is particularly awkward for relatively shallow and narrow panels for which the ultimate load well may exceed the bifurcation buckling load.

A possible procedure may begin with optimization of the perfect structure with the bifurcation buckling load as a constraint. Subsequently a knock-down factor for the optimized structure is established through nonlinear analysis with random imperfections. The analysis is repeated for a sequence of values of the bifurca-

tion buckling load constraint, so that the range of computed values of the ultimate load covers the range of load levels for which optimum designs are desired. In this way a structure is obtained that will carry the design load. However, the imperfection sensitivity is only used to shift the load range corresponding to a family of design configurations. The imperfection sensitivity has no direct influence on the choice of the design configuration. The approach taken here is to leave one decision variable to be determined on the basis of the final nonlinear analysis. It appears from Figure 1, for example, and from the results presented in Reference 8, that the parameter with the greatest effect on the knock-down factor is the ratio between local and general instability loads. An approach in which this factor is allowed to influence the optimum design is illustrated in Figure 5.

First a set of values of the constraint on local buckling ϕ and a set of load factors λ_o are chosen. Note that λ_o does not represent the load carrying capability of the imperfect panel. The sequence of values of λ_o represent a trial range within which the actual critical load factor (limit load) for the imperfect panel is expected to be found. The perfect panel is optimized with the bifurcation buckling constraint for each of the $\phi(i)$, $\lambda_o(i)$ combinations. With M different values of ϕ and N different values of λ_o we obtain M x N different panel designs. For each of these a set of K imperfection configurations (K = 10 to 20) are chosen by a random procedure. For each panel K nonlinear analyses, with strain constraints or other failure criteria, are then carried out. As a consequence we obtain N x M sets of K limit loads λ_{imp}. These data can be plotted and cross plotted as shown in Figure 5. Figure 5a shows plots of probability-of-failure versus the limit load λ_{imp} for two values of the trial load λ_o, $\lambda_o^{(1)}$ and $\lambda_o^{(2)}$, and three values of ϕ. Since each combination of λ_o and ϕ corresponds to a fixed design, we also know the structural weight corresponding to each curve. We can determine by statistical analysis for each λ_o, ϕ combination the value of the limit load factor λ for which we have less than one percent (for example) risk of failure. Then, for each selected value of ϕ we have M points on curves such as those shown in Figure 5b. By cross plotting, Figure 5c, we can, for any load factor within the range, obtain a curve showing the panel weight as a function of the local buckling parameter ϕ. For any desired limit load level we select the value of ϕ corresponding to the minimum.

For any λ_o,ϕ combination the design parameters are known from the optimization in the second (ECHO) phase. Consequently, after an optimum value of ϕ has been

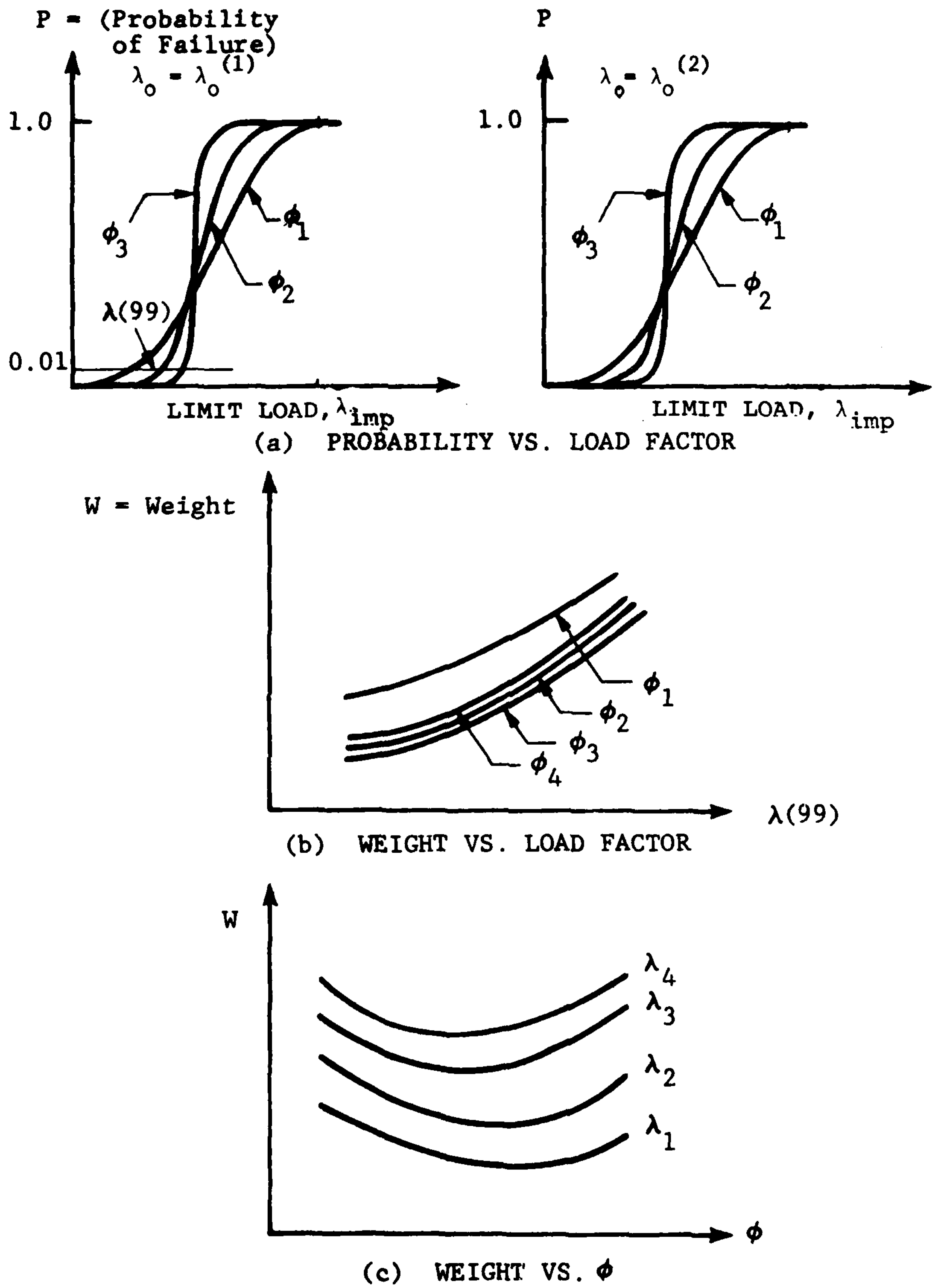

Figure 5 Optimization of Imperfect Panels

selected these parameters can be plotted versus the limit local factor λ and for any value λ_i in the range covered, optimum dimensions can be read from the plots.

The number of times a constraint function has to be determined during optimization varies with the number of decision variables. Typically it may converge on a design after some one to two hundred function values have been determined. In that case the procedure outlined above reduces the number of times a nonlinear analysis is required by a factor of ten or so. Still with $M = N = 4$ and $K = 15$ we need 240 nonlinear analyses. With the present procedure we have the additional bonus that the optimum design is obtained for a number of load levels. This would be quite beneficial, for example, in the design of an airplane wing in which the loading intensity varies over the surface.

It may be noticed also that the procedure outlined is not applicable only in the case of evaluation of imperfection effects. It can be used in many cases when computation of the buckling load requires excessive computer time. For example, stiffened panels can be optimized with the assumption of smeared stiffeners and with cross-section deformation neglected. The analysis just described can be used to account for cross-section deformation and shear-lag effects. In those cases the stiffener spacing may take the place of ϕ as the parameter to be determined in the a posteriori analysis.

Figure 6 shows the procedure in a block diagram. The design specifications include choice of material, minimum gages, type of stiffening (load distribution, etc.). A program for initial sizing (1) may be based on either the simultaneous mode approach or the mathematical programming approach utilizing simple approximate explicit solutions for stability constraints. The initial design can be refined in the "perfect panel optimization" box (2). The effects of imperfections are accounted for in the a posteriori analysis (3). The figure indicates that the optimization process runs through the three phases sequentially for each λ_o, ϕ combination. This is not necessary but the design parameters corresponding to an array of λ_o, ϕ combinations can be written on a file at the end of the analysis phase (1) or (2). The subsequent phase reads input data from this file.

It is clearly feasible to derive executive software such that the entire sequence

OPTIMIZATION IN THE PRESENCE OF
RANDOM IMPERFECTIONS

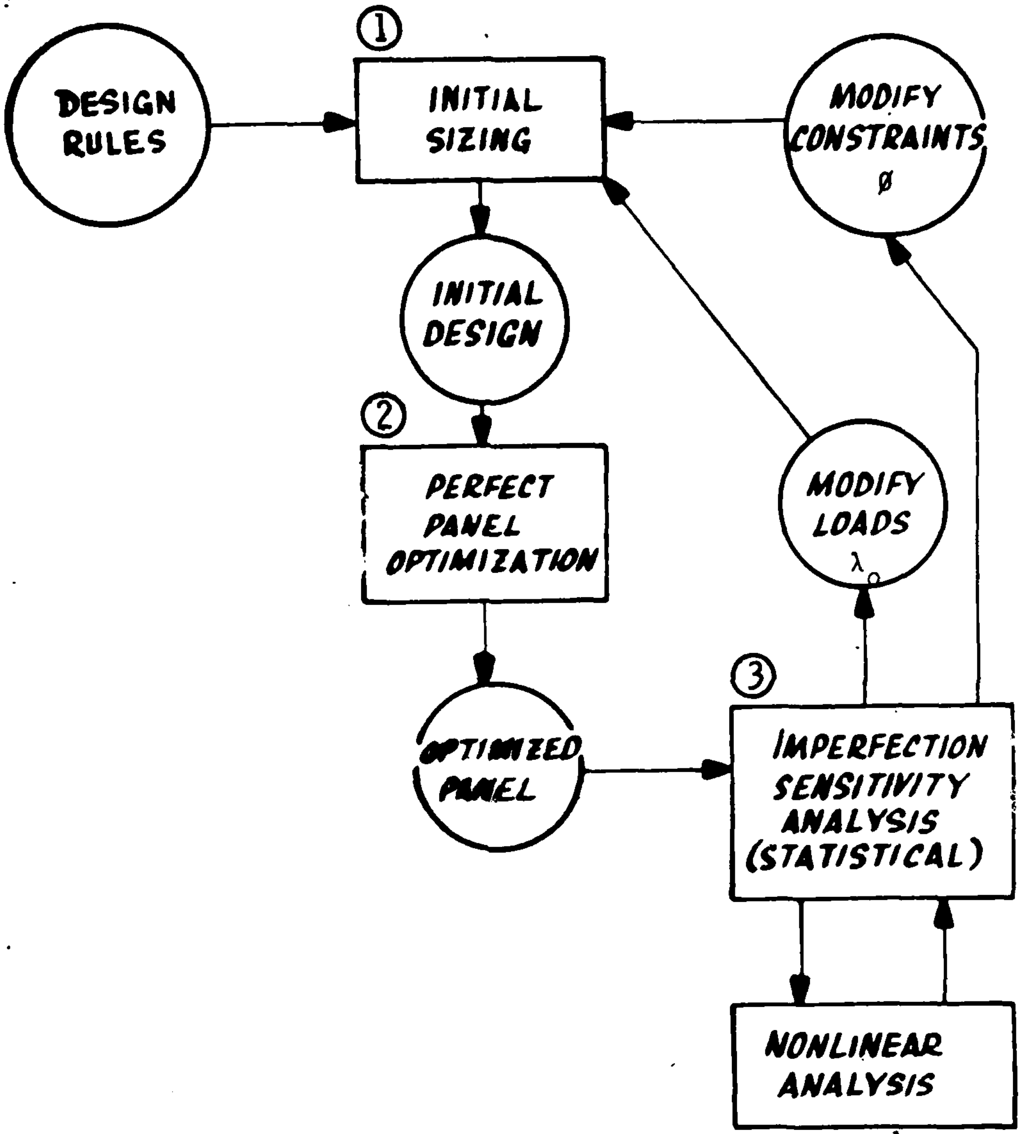

Figure 6. Optimization Procedure

from initial sizing to statistical analysis of the nonlinear analysis results can be performed without interference by the analyst. However, for a number of reasons this does not seem practical. The initial sizing is most conveniently performed in the interactive mode while the second and third phases involve use of programs with storage requirements beyond those available for interactive analysis at AFFDL. Further, it seems likely that the analyst would like to inspect the results from computations in one phase before he proceeds to the next. The design arrived at may exhibit some undesirable features and as a consequence a restart with different constraints is required. The weight in the initial phase may be high in comparison to alternative configurations so that further pursuit is meaningless. Finally, if separate programs or program complexes are provided for the three phases, it is easier to use the same program for special functions that do not utilize the full range of the computational system. A slight disadvantage in going through three different phases in the optimization procedure is mitigated by the fact that software for later phases can read as input the output files from an earlier analysis phase. In this way the input that the user has to define as he enters a new phase is minimized.

Section VI

THE POIS PROGRAM

The POIS Program allows its user to perform weight optimization of structural panels under stability constraints. The optimization can proceed in three separate phases. Progress from one phase to the next implies increasing accuracy in computation of the critical load and as a consequence increasing computer cost. The first phase (PANDA) can be conceived as a program for initial sizing. The second phase is referred to by the code name ECHO. In this phase the constraint is still the bifurcation buckling load of panels with perfect geometry. The nonlinear analysis of imperfect panels, the third phase, can be carried out in ECHO or deferred to RRSYS for more complex cases.

In the interest of economy an additional user option has been introduced. The geometric imperfections can be simulated through the application of random normal forces to the panel. In a nonlinear analysis with user-defined displacement functions the major part of the computer time is spent on the computation of the

coefficients in the reduced system. Since these coefficients are functions of the initial geometric imperfections they must be recomputed each time before the reduced system can be integrated. Therefore, the analysis becomes much less expensive if the imperfections are simulated by use of normal forces rather than by geometric deviations from the true shape. The program user defines a "quality parameter". A routine in RRSYS or ECHO then defines the normal loading in the form of a Fourier series with random coefficients. Each coefficient in this series is independently determined as the product of the quality parameter and a random number with uniform probability in the range -1 to +1. During integration of the reduced system the normal loads are held constant while the inplane loading is gradually increased.

SUMMARY OF PANDA

A detailed description of PANDA with instructions for its use is given in Volume 1 of Reference 9.

Objective

The objective of the development of PANDA has been to create a practical, interactive computer program which derives minimum weight designs of stiffened cylindrical panels under combined in-plane loads, N_x, N_y, and N_{xy}. The loading of the stiffened panel is assumed in most cases to result in uniform membrane strain components ε_x and ε_y in both skin and stiffeners and uniform shear strain γ_{xy} in the skin.

Buckling loads are calculated by use of simple assumed displacement functions. For example, general instability of panels with balanced laminates and no shear loading is assumed to occur in the familiar $w(x,y) = C \sin(ny)\sin(mx)$ mode. The skin is cylindrical with radius R and the stiffeners are composed as assemblages of flat plate segments the lengths of which are large compared to the widths and the widths of which are large compared to the thicknesses. These flat plate segments are oriented either normal or parallel to the plane of the panel skin.

Material Properties

If the material is orthotropic or anisotropic, buckling is assumed to occur at stress levels for which the material remains elastic. Feasible designs are constrained by maximum stress or strain criteria. Plasticity with arbitrary strain hardening is permitted if the material is isotropic. The cylindrical skin and stiffener segments can be composed of multiple layers of isotropic or orthotropic material. Each layer has a unique angle of orthotropy relative in the case of the panel skin to the direction of the generator (x-direction) and in the case of a stiffener segment to the stiffener axis. In the buckling analysis, the segments of the stiffeners are assumed to be monocoque and isotropic or orthotropic, not layered anisotropic. Therefore, equivalent orthotropic properties for stiffener segments are calculated from input data for the stiffener segment laminates provided by the program user.

Types of Buckling

Optimum designs with respect to weight are obtained in the presence of constraints due to local and general buckling, maximum tensile and compressive stress or strain, maximum shear strain, and lower and upper bounds on skin layer thicknesses, stiffener cross section dimensions, and stiffener spacings. Design parameters which are allowed to vary during the optimization phase include panel skin laminae thickness and winding angles, spacings of stiffeners, and thicknesses and widths of the segments of ring and stringer cross sections.

The buckling formulas are derived from Donnell's theory, followed by <u>a posteriori</u> application of a reduction factor $(n^2 - 1)/n^2$ for panels in which the axial half wavelength of the buckling pattern is longer than the panel radius of curvature, R. The circumferential wave index equals $n\pi R/b$ or $n\pi R/b_o$ with n being the number of half waves in the circumferential direction over the spans b or b_o, respectively, where b is the width of the panel and b_o the stringer spacing.

Local Buckling

The different buckling constraints represent general instability as well as local buckling. The local buckling constraints include skin buckling as well as various stiffener buckling modes discussed in Volume 1 of Reference 9. It is permissible to use different load levels as constraints for local and general instability.

Optimization

The computer program CONMIN (References 10,11) is used for determining the minimum weight design of the panel. This program, written by Vanderplaats in the early 1970's, is based on a nonlinear constrained search algorithm due to Zoutendijk (Reference 12). The basic analytic technique used in CONMIN is to minimize an objective function (panel weight, for example) until one or more constraints, in this case buckling loads, maximum stress or strain, and upper and lower bounds on design variables, become active. The minimization process then continues by following the constraint boundaries in the design variable space in such a direction that the value of the objective function continues to decrease. When a point is reached at which no further decrease in the objective

function is obtained, the process is terminated.

SUMMARY OF ECHO

A detailed description of ECHO with instructions for its use is given in Volume 2 of Reference 9.

Objective

The objectives of the development of ECHO were to permit optimization of panels with a variety of geometries, boundary conditions, and constraints which include a mode separation parameter (ϕ); and to provide a means whereby nonlinear analysis can be executed from data obtained in the optimization phase. The ECHO system was developed with the following as important guidelines:

1) control of operations by analyst
2) use of existing structural and optimization modules
3) ease of modification and extension
4) efficiency with respect to computer time.

Stiffeners and Wall Construction

Rings and stringers are modeled in ECHO as assemblages of flat segments each of which can be rotated by a given angle and which are joined together in a prescribed manner to generate stiffener types such as a blade, T, J, hat, corrugation, etc. Skin and stiffeners may consist of multiple layers of orthotropic materials. A layer (lamina) is defined by a thickness, material orientation angle (winding angle) and material type. In a design problem (optimization) the stiffener segment widths, layer thicknesses, and material angles can be design variables. Provision is made to reduce the number of design variables by linking (generation of a set of linear equations which relate some design variables to other design variables).

The advantages of ECHO over PANDA are:

Arbitrary boundary conditions may be specified on each of the four edges of the panel, including simple support (antisymmetric), fixed, free, and symmetry.

Arbitrary buckling modes can be defined. The buckling modes may be produced by general computer programs such as STAGSC-1 or VIPASA. If STAGSC-1 is used the program will define a local buckling model separate from a discrete stiffener model. For computer economy it appears necessary to use a model with smeared stiffeners for general instability. While VIPASA gives good economy and accurate buckling loads, it has the disadvantage that only simply supported panels with stiffeners in one direction can be considered. Also, the program does not distinguish between general and local buckling modes. A program, FRITZ, based on the expansion of the displacement components in Fourier series, has been developed under the present contract and is included in ECHO. This gives freedom to the user to define several components in a buckling mode. The stiffeners can be considered as discrete elements. (Use of smeared stiffeners may yield buckling loads corresponding to general instability modes that are as much as 40 per cent too high.) It is envisioned that FRITZ will be used in the actual optimization procedure, while STAGSC-1 and VIPASA will be used primarily to verify selected results from FRITZ. The FRITZ program also includes a capability to perform nonlinear analysis.

Layer thicknesses and winding angles of laminae in stiffener segments may be used as decision variables in the optimization process.

Stiffener cross sections need not be open sections and the individual segments of which the stiffener cross sections are composed need not be parallel or perpendicular to the plane of the panel skin at the stiffener line of attachment.

Optimization

As in PANDA, CONMIN is used as optimizer. However, in addition, provisions have been made in ECHO for inclusion of an optimizer (ALMIN) with the potential of greater efficiency than CONMIN (Reference 13). However, more experience in its use is needed before it can be applied in engineering analysis.

Operation of ECHO

In the ECHO package, a program called ECHO is used to provide input data. A program called OEXEC is used to perform operations for the optimization problem.

At present, the structural analyzers in the ECHO package include STAGSC-1, SFRITZ (STAGS Functional Rayleigh-Ritz), FRITZ (Functional Rayleigh-Ritz), and VIPASA (Reference 14), which is embedded in the program PASCO (Reference 15). Other structural analyzers and optimizers can be included in the ECHO system without extensive programming.

STAGS

STAGSC-1 is the most recent version of the STAGS series of computer programs. It provides options for linear and nonlinear static stress, stability, vibration, and transient analysis of general shells. The program is based on the finite element method and is described in some detail in Reference 16. STAGSC-1 consists of two processors STAGS1 and STAGS2. STAGS1 is a preprocessor which reads the input and generates some intermediate results needed for the final structural analysis in STAGS2. In ECHO, the linear bifurcation buckling option with uniform prestress is used to obtain eigenvalues to represent the buckling constraints. The use of STAGS in ECHO provides generality with respect to the geometry, loads, and boundary conditions of the structural configuration to be optimized. However, in optimization, with the eigenvalue analysis repeated a large number of times, the straightforward finite element analysis in STAGSC-1 sometimes leads to excessive computer time. Greater computational efficiency can be achieved by use of the programs SFRITZ and FRITZ.

VIPASA is a computer program for bifurcation buckling and vibration analysis of prismatic structures. VIPASA will handle an arbitrary assemblage of thin, flat, rectangular plate elements. The laminates of each plate element must be symmetric. The panel edges are assumed to be simply supported at the transverse edges with the loading uniform along the panel length. The buckling pattern is therefore sinusoidal in the axial direction. Solutions of the differential equations for buckling of plates are obtained and undetermined coefficients are computed from the compatibility conditions between adjacent plate elements. Rings cannot be included. Shear buckling is obtained in an approximate manner. VIPASA does not distinguish between local and general instability, but calculates mode shapes rigorously, as would a finite element program. Thus, modes corresponding to general instability with local perturbations due to stringers are calculated by VIPASA. In ECHO, program PASCO, which contains VIPASA and CONMIN in subroutine

form, can be used directly for a simple buckling analysis of a given configuration or for an optimization analysis.

SFRITZ, meaning "STAGS Functional Rayleigh-Ritz", is a computer program for bifurcation buckling analysis of flat or curved rectangular panels. It is based on a combination of Rayleigh-Ritz techniques and finite element discretization. Trigonometric basis functions selected by the user determine displacement and rotation values at nodes of the finite element model. The buckling pattern is represented as a linear combination of these element basis functions. The finite element integration is then used to convert the buckling problem of STAGSC-1 to a reduced system with the user selected basis functions as the generalized degrees of freedom. Buckling is considered for axial compression, hoop compression, shear or any combination of these cases. It may be noted that SFRITZ is not restricted to simple structures or boundary conditions and may be applied to any elastic structure within the domain of STAGSC-1.

FRITZ provides buckling and non-linear collapse analysis for flat or curved rectangular panels by use of Rayleigh-Ritz functional methods. As with SFRITZ, the user selects trigonometric functions as the basis functions for the analysis. A discrete grid is also defined for the panel as in a STAGSC-1 model. However, energy integration in FRITZ proceeds by direct numerical computation using the trigonometric functions instead of the finite element discretization and shape functions used in SFRITZ or STAGSC-1.

In general, the direct Rayleigh-Ritz analysis used in FRITZ achieves much greater economy than a corresponding finite element analysis and is thus particularly suited for the study of imperfection sensitivity of panels.

The choide of trigonometric functions to be included in the basis vector space is controlled by the user. The user has options to define normal as well as inplane displacement functions or to define normal displacements only. In the latter case, corresponding inplane displacements are computed from the nonlinear inplane equilibrium equations. While SFRITZ can be applied to very general structures, FRITZ can at present only be used for analysis of flat or curved panels of rectangular plan form. The use of numerical integration, however, permits the treatment of various boundary conditions and loadings.

SUMMARY OF RRSYS

A detailed description of RRSYS is given in Volume 2 of Reference 9.

RRSYS is a system of computer programs featuring the use of global functions for approximation of the displacement field. It consists of an executive program and a number of subprograms. The functions within the scope of the system can be executed in a batch mode by way of user-written procedure files. A library of hardwired functions is available for user convenience. The main purpose of the RRSYS system is to make nonlinear analysis with STAGSC-1 more economical. This goal is achieved through integration in a reduced space (the global function space) for extrapolation yielding good initial estimates of displacements at subsequent load steps. A Rayleigh-Ritz analysis used in conjunction with an auxiliary finite element model allows accuracy control and automatic generation of global functions. The RRSYS system also includes an option in which the user defines the reduced solution space, i.e., the user defines a set of basis functions for the Rayleigh-Ritz analysis. In that case, the generation of global functions and accuracy control are exercised by the program user.

For more complex structures, the option for user-written functions may prove too difficult, but for structural panels, it is relatively easy to define a suitable set of basis functions such as trigonometric series. The computer run time with user-written functions is a fraction of the run time in a finite element analysis. As a consequence, this option is most suitable for use in a study of geometrically simple structures.

Under the present contract, FRITZ was integrated into RRSYS. A procedure file was added which calls for the computations required in the third phase of optimization of imperfection-sensitive structures. That is, the output files from ECHO can be read in and processed in sequence, as required in the last phase of the optimization.

Section VII

NUMERICAL RESULTS

The POIS program has been applied in optimization of five different panels, three flat panels and two cylindrical. The basic configurations of these flat panels are shown in Fig 7. As indicated, the material properties of the three flat panels are typical for aluminum. The two curved panels (4B, 4J), one with blade and one with J-stiffeners, were made of composite material. The layup in the skin was in both panels fixed as indicated in the figure.

For the first example a very wide flat panel with blade stiffeners was considered. The reason for this choice was that a panel of this type would most closely resemble the case considered in Reference 1. After optimization with PANCON, preliminary ECHO-analysis based on PASCO disclosed a substantial difference between results from PANCON and STAGSC-1 with smeared stiffeners, which agree, and the more accurate results from PASCO. The reason for this discrepancy is that the general instability mode for such a short panel is far from a smooth half-sine-wave, as assumed in PANCON. Bifurcation buckling modes for the same panel obtained with BOSOR 4 (Reference 17) are shown in Figure 8. The waveforms observed do not include a clean wide column buckling mode and thus makes the analysis of Reference 1 somewhat questionable. A good approximation of the waveforms shown in Figure 8 can readily be defined by the FRITZ input.

In optimization studies with FRITZ as the structural analyzer, the user decides whether a model with smeared stiffeners or one with discrete stiffeners is to be used. For local buckling the user can include the skin only, simply supported at the stiffener attachment lines or define a model including skin and stiffeners. The stiffeners can also be modeled as plates, simply supported at the intersection with the skin.

For buckling analysis, general or local, the user defines a number of components in a trigonometric series defining the eigenmodes. Normal and inplane displacement components can be defined separately or the user can define the normal displacement components and request that corresponding inplane displacement be automatically computed from the inplane equilibrium equations. Exploratory analysis with PASCO (i.e., VIPASA) or STAGSC-1 are helpful in selection of these terms, and are finally used to verify the validity of the chosen buckling modes. Results from the

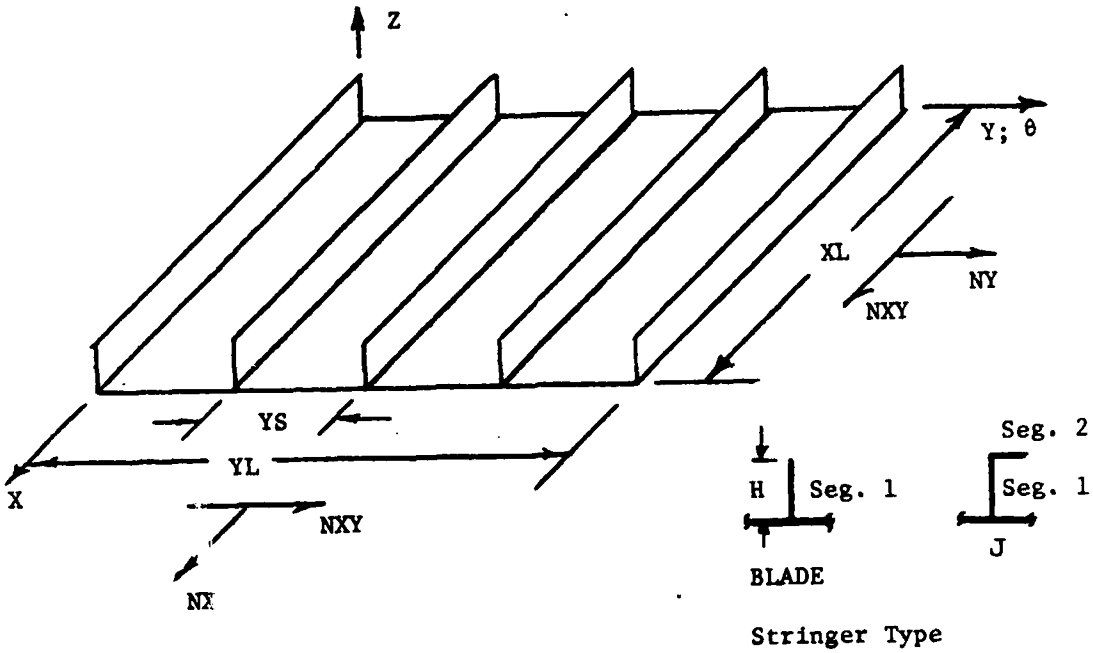

CASE NO	PANEL TYPE	LENGTH XL (IN)	WIDTH YL (IN)	MAT. NO	WALL NO	STRINGER TYPE	SPACING YS (IN)	MAT. NO	WALL NO SEG 1	WALL NO SEG 2	LOAD NO
1	FLAT	10.0	60.0	1	1	BLADE	15.0	1	1	-	1
2	FLAT	10.0	60.0	1	1	BLADE	7.5	1	1	-	1
3	FLAT	40.0	60.0	1	1	BLADE	7.5	1	1	-	2
4B	CURVED	30.0	24.0*	2	2	BLADE	6.0	2	2	-	3,4
4J	CURVED	30.0	24.0*	2	2	J	6.0	2	2	3	3

* RADIUS=80.0 IN

MATERIAL PROPERTIES

MATERIAL NUMBER	E11 (MPSI)	E22 (MPSI)	G (MPSI)	NU	RHO (LB/CU IN)
1	10.0	10.0	3.846	0.3	0.1
2	23.0	1.7	0.94	0.304	0.056

WALL LAYERING

WALL NO	NUMBER OF LAYERS	LAYERING-ANGLE (DEGREES)
1	1	0
2	16	(90/±45/0/0/∓45/90)S
3	17	(90/±45/0/0/∓45/90/0,N)S

LOAD SETS

LOAD NO	LOADS IN (KIPS/IN)
1	NX=-16.0,-8.0,-4.0,-2.0
2	NX=-8.0,-6.0,-4.0,-2.0
3	NX=-3.0;NX=-3.0,NXY=1.0
4	NX=-8.0,-6.0,-4.0,-3.0

( )S - SYMMETRIC LAYERING
0,N - 2N LAYERS AT 0 DEGREES TREATED AS ONE LAYER

Figure 7 Description of stiffened panels

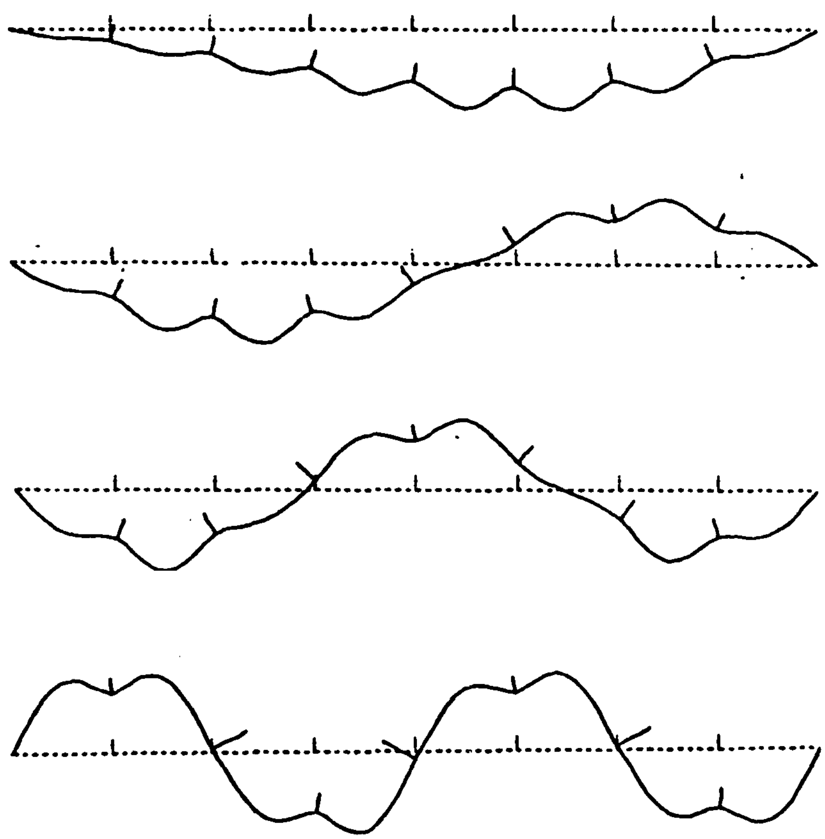

Figure 8 Buckling Modes for Case 2

(ϕ = 1.0, N_x = -16.0 KIPS/in.)--BOSOR Analysis

example cases are presented in the Appendix. A brief discussion of these results follows.

Cases 1, 2, 3: PANDA analyses indicated that with smeared stiffeners, the mode shape for general instability was one axial and one transverse half wave ($m = n = 1$) and that buckling of the panel between stiffeners has one transverse half wave ($n = 1$) and one axial half wave ($m = 1$) for Cases 1, 2 and five half waves ($m = 5$) for Case 3. PASCO analyses (with $\phi = 1.0$) showed that the buckling load was substantially less than that given by PANDA. For Case 2 the ratio was about 0.73. The buckling mode has one half wave in the axial direction. The deformation mode in the transverse direction is not given by PASCO. Analyses with STAGSC-1 and BOSOR4 revealed the mode shape indicated in Figure 8. The BOSOR4 buckling load agrees very well with that predicted by PASCO. The form of this normal displacement is closely approximated by:

$$f(y) = a_1 \; 1 - \cos(2N\bar{y} \;) \; \sin \bar{y} + a_2 \sin \bar{y}$$

in which $\bar{y} = \Pi y/L$, N is the number of stringer spacings, and a_1 are undetermined coefficients. By use of the relation:

$$\cos(2N\bar{y})\sin \bar{y} = \frac{1}{2} \{\sin [(2N + 1)\bar{y}] - \sin [(2N - 1)\bar{y}]\} \quad ,$$

f(y) can be written in the form:

$$f(y) = a_1 \sin \bar{y} + a_2 \sin[(2N+1)\bar{y}]+a_3 \sin[2N-1)\bar{y}]$$

which can be directly defined in FRITZ.

The panel dimensions and the corresponding weights are shown in Figures 1A through 6A and in Tables 1A through 3A in the Appendix. It should be noted that the lower bound on the blade thickness (T2) was changed in the ECHO analyses from 0.1 in. used in PANDA to 0.04 in.

Case 4: A PANDA analysis of Case 4B with $\phi = .2$, $N_x = 3.0$; $N_{xy} - 1.0$ kips/in. gives a general instability mode with one axial half wave and two circumferential half waves ($m = 1$; $n = 2$). The local mode between stringers is $m = 5$; $n = 1$. For Case 4J, $\phi = .2$, $N_x = -3.0$ kips/in., PANDA gives the same mode shapes as

those in Case 4B. For both these cases PANCON was only run for one ϕ,λ_o combination. In the ECHO analysis results (values of design variables) for one λ_o,ϕ combination were used as starting values for the next.

In Cases 4B, 4J under axial load only two general instability modes are used m,n=1,1 and 1,2 and one local mode m,n=5,1 is used for bluckling of the panel between stringers. Analyses of the optimized panels show that for all ϕ-values the eigenvalues for the mode m,n = 1,1 are lower than for mode m, n = 1,2 when N_x = -8,000. At N_x = -6,000, the eigenvalues for the two modes are about equal and for lower values of the load the mode m,n = 1,2 is critical.

When shear is added to the load system, additional modes are introduced. It is suggested in Reference 18 that only modes in which m + n is even need to be included. This was verified in a few analyses with FRITZ. For Cases 4B and 4J with axial load and shear the following six terms are used to approximate the mode for general stability analysis:

m,n = 1,1; 3,3; 2,2; 1,3; 3,1; 1,2.

The analysis of local buckling was based on a model of the skin between two stiffeners, simply supported at the edges. With the wave numbers now referring to the dimensions of this model the following 13 terms were included:

m,n = 1,1; 3,3; 2,2; 1,3; 3,1; 4,4; 4,2; 2,4; 5,5;
5,1; 1,5; 5,3; 3,5.

The reason that so many terms need to be included in the local stability analysis is the less favorable aspect ratio of the panel (between stiffeners).

Nonlinear analyses were performed only in Case 4B, the blade stiffened panel subjected to axial compression. For each configuration the failure load was computed with 10 randomly determined imperfections. For computer economy the imperfections were simulated with random loads. It was assumed that the stiffeners would be only slightly bent at the critical load level and, therefore, that the general instability modes would be close to a half-sine-wave form in the axial

direction. Only two general instability modes with normal displacements were included, one with one half wave and one with two half waves in the circumferential direction. In addition it is necessary to include modes with only inplane displacements to approximate the plane strain field in the skin corresponding to the forces transferred from the eccentric stiffeners. The amplitude of these functions may be related to the amplitude of corresponding lateral displacement modes in a linear analysis. In a nonlinear analysis with buckling skin, the position of the effective neutral surface is unknown and, thus, the amplitudes of the general inplane displacement modes are freedoms of the system. A total of eight modes were used, a number that easily can be increased if the demand for accuracy so requires.

The nonlinear analysis was performed in ECHO, using the nonlinear option in the FRITZ program. For each combination of ϕ and λ_o (5 ϕ-values and 4 λ_o-values) a total of 10 nonlinear analyses with random imperfections were performed in which the axial load was gradually increased until failure was indicated.

The critical load is assumed to be reached when the load displacement curve exhibits a maximum or whenever the fracture criterion is violated. As it turned out, only in one case out of 200 did the panel fail at a limit point in the load-deflection curve. Fracture was assumed to occur if any one of the following conditions was violated:

$$.009565 > \varepsilon_L > -.007826$$

$$.003200 > \varepsilon_N > -.012350$$

$$.016860 > \gamma > -.016860$$

where ε_L and ε_N are the strains parallel and normal to the fibers and γ is the shear strain.

The statistical analysis of the results from the nonlinear analysis is presented in Table 5A in the Appendix. The "INPUT DATA VALUES" are the ultimate loads computed for a sequence of independent random imperfections for the ϕ,λ_o values as indicated by "PHI" and "N" in the heading. With the "base load" equal to -1.0 lbs/in λ_o and N are used interchangeably. The data in all cases were treated

with the assumption of a normal probability distribution. The critical load was defined as the low 99 per cent probability level. Optimum design is to be determined for panels carrying ultimate loads corresponding to $\lambda = 3000$, 4000, and 5000, i.e., $N_x = -3.0$, -4.0, and -5.0 kips/in. In order to obtain such data a set of values of λ_o were chosen in the range $3000 \leq \lambda_o^{(i)} \leq 8000$. The upper part of Figure 10A shows the limit loads $\lambda(99)$ as functions of ϕ for a set of λ_o-values in this range. The curves probably would be smoother if more than 10 cases had been included for each parameter combination. This can easily be done since the nonlinear FRITZ analysis in this case requires very little computer time. The lower part of Figure 10A (corresponding to the final curves in Figure 5 i.e., ^{5}c) shows the panel weight as a function of ϕ for the three levels of ultimate load corresponding to a 99 per cent probability design. There is no minimum in the range, but the minimum values on plate thickness and stringer spacing precludes use of ϕ-values lower than 0.2.

The indication is clearly that the optimum design is one in which the skin is allowed to buckle well before the ultimate load is reached. For the lowest stress level, the weight corresponding to $\phi = 1.0$ is about 67 per cent higher than that for $\phi = 0.2$. This tendency is well established even if some doubts may be cast on the statistical analysis. As shown in Table 5A ($\phi = 0.8$ and N (or λ_o) = 4000, for example) there is a clear tendency towards two separate probability distributions. This tendency may be representative of actual structural behavior or it may be due to an idiosyncrasy in the definition of the imperfections. Only a carefully executed series of experiments can answer such questions and allow continued progress in this matter.

Section VIII

CONCLUSIONS

A complex of computer programs with the code name POIS (Panel Optimization with Integrated Software) has been developed for optimization of structural panels. The effects of initial imperfections are taken into account in the design procedure. This has become possible because a very efficient program module FRITZ (Functional RITZ-analysis) was developed for nonlinear analysis of panels with random imperfections. Five different panels were optimized in order to demonstrate the validity of POIS. Nonlinear analyses with STAGSC-1 of selected designs indicated that the type of failure at a limit point typical for infinitely wide stiffened panels (Reference 1) was unlikely to occur for panels of finite width with support along longitudinal edges. Rather, such panels, more typical for aircraft design, appear to have some postbuckling strength.

Only for one panel design was the whole scope of POIS exercised. In that case, the nonlinear analysis results were treated statistically and optimum designs of imperfect panels were established. It can be concluded from this analysis that the critical loads show considerably more scatter if the panels are lightly loaded and also if local and general instability loads are simultaneous. For ϕ-values less than 1.0 local buckling occurs before general instability load and even for the perfect structure the ratio between the actual critical load, represented by λ; and the "Euler load", corresponding to λ_0, will be less than unity. Consequently the ratio λ/λ_0 indicates the degree of imperfection sensitivity only if $\phi = 1.0$. For that case $\lambda(99)/\lambda_0$ varies between 0.63 and 0.85 for the different load levels, i.e., the imperfection sensitivity is notable.

The results indicate that the most effective design is obtained if local buckling is permitted to occur well below the design load. Clearly, the success of optimization with POIS depends on a capability to define the parameters governing the random imperfections. As a consequence, it is felt that any further progress in this area will be possible only if the effort is augmented with a carefully executed experimental program.

Section IX

REFERENCES

1. Koiter, W. T. and Skaloud, M., "Interventions in Comportement Postcritique des plaques Utilisees en Construction Metallique," Colloque intern. a 'Universite' de Liege, 1962.

2. Bridget, F. J. , Jerome, C. C., and Vossler, A. B., "Some New Experiments on Buckling on Thin-Wall Construction, " ASME Transactions, V. 56, 1934.

3. Thompson, J. T. M. and Lewis, G. M., "On the Optimum Design of Thin-Walled Compression Members," J. Mech. Phys. Solids, 1972.

4. Van der Neut, A., "The Interaction of Local Buckling and Column Failure of Thin-Walled Compression Members," Proc. 12. Int. Congr. Appl. Mech., Stanford University, Springer, 1968.

5. Tvergaard, V., "Imperfection Sensitivity of Wide Integrally Stiffened Panel Under Compression," Center Appl. Math. and Mech., U. of Denmark, Report No. 19, 1971.

6. Budiansky, B. and Hutchinson, J. W., "Buckling: Progress and Challenge," Trends in Solid Mechanics 1979, Delft U. Press, June 1979.

7. Koiter, W. T., "On the Stability of Elastic Equilibrium (in Dutch), thesis, Delft, H. J. Paris, Amsterdam, 1945. English Translation, Air Force Flight Dyn. Lab. Tech. Rep., AFFDL-TR-70-25, Wright Patterson Air Force Base, Ohio, 1970.

8. Koiter, W. T. and Pignataro, M., "An Alternative Approach to the Interaction between Local and Overall Buckling in Stiffened Panels," in Buckling of Structures, Springer, 1974.

9. Bushnell, D., Stern P., Almroth, B. O., and Stehlin P., "Panel Optimization by Integrated Software; POIS," Air Force Flight Dyn. Lab., Tech. Rep. AFFDL-TR-XX-XX, Wright Patterson Air Force Base, 1981.

10. Vanderplaats, G. N., and Moses, F., "Structural Optimization by Methods of Feasible Directions", National Symposium on Computerized Structural Analysis and Design, Washington, D.C., March 1972.

11. Vanderplaats, G. N., "CONMIN - A FORTRAN Program for Constrained Function Minimization; User's Manual", NASA TM X-62, 282, Ames Research Center, Moffett Field, CA, August 1973; Version updated in March 1975.

12. Zoutendijk, G., Methods of Feasible Directions, Elsevier Publishing Corp., Amsterdam, 1960.

13. Jensen, P. S., and Loden, W. A., "Supplementary Studies on the Sensitivity of Optimized Structures", Air Force Flight Dyn. Lab., Tech. Rep. AFWAL-TR-81-3013, March 1981.

14. Wittrick, W. H., and F. W. Williams, "Buckling and Vibration of Anisotropic or Isotropic Plate Assemblies Under Combined Loadings," International Journal of Mechanical Sciences, Vol. 16, pp. 209-239 (1974).

15. Stroud, W. J. and Anderson, M. D., "PASCO: Structural Panel Analysis and Sizing, Code-Capability and Analytic Foundations", NASA TM 80181, January 1980.

16. Almroth, B. O., and Brogan, F. A., "The STAGS Computer Code", NASA CR 2950, February 1978.

17. Bushnell, D., "Stress, Stability and Vibration of Complex, Branched Shells of Revolution", Computers and Structures, Vol. 4, pp. 399-435, 1974.

18. Timoshenko, S., Elastic Stability, McGraw Hill, New York, New York.

Appendix A

NUMERICAL RESULTS

This Appendix contains results of optimization and nonlinear imperfection analyses described by Figure 6. The optimization results include total panel weight and values of the decision variables as a function of the parameter ϕ and design loads. The nonlinear analysis results for Case 4D include failure load and weight as a function of ϕ and design loads. Following are comments on optimization variables.

CASES 1-3: Stiffener height (H), and thicknesses (T1, T2), are design variables. T1 is the total panel thickness and T2 is the total blade thickness. In the PANDA analyses, the lower bounds on T1 and T2 are 0.04 and 0.10 in. whereas in the ECHO analyses, these lower bounds are both 0.04 in.

CASE 4B: Stiffener height (H) and Thicknesses (T1, T2) are design variables. T1 is the single layer thickness of the panel and T2 is the single layer thickness of the blade stringer. All layers of the panel have a thickness T1 and all layers of the blade have a thickness T2. Thus, the total thickness of the panel and blade are 16·T1 and 16·T2. The lower bound on a layer thickness is 5 mils.

CASE 4J: Design variables H, T1, T2 are defined as in Case 4B. The flange width (Segment 2) of the J stiffener is linked to the width (H) of Segment 1 so that the flange width is one half of the height (H). The flange has the addition of ten (10) 0 degree orientated layers which makes the total thickness 16·T2 + 0.05.

CASE 1 PANDA

-NX (KIPS/IN)	PHI	WEIGHT (LBS)	T1 (IN)	T2 (IN)	H (IN)
16.0000	1.0000	26.8800	0.4354	0.1333	1.4150
16.0000	0.8000	25.0200	0.4036	0.1320	1.5100
16.0000	0.6000	22.7900	0.3662	0.1268	1.6110
16.0000	0.4000	19.9800	0.3194	0.1179	1.7220
16.0000	0.2000	15.9300	0.2527	0.1017	1.8860
8.0000	1.0000	21.2600	0.3461	0.1000	1.2340
8.0000	0.8000	19.7800	0.3209	0.1000	1.3160
8.0000	0.6000	18.0200	0.2912	0.1000	1.3800
8.0000	0.4000	15.8100	0.2539	0.1000	1.4470
8.0000	0.2000	12.6400	0.2007	0.1000	1.5050
4.0000	1.0000	16.8700	0.2747	0.1000	0.9786
4.0000	0.8000	15.7000	0.2547	0.1000	1.0440
4.0000	0.6000	14.3000	0.2311	0.1000	1.0960
4.0000	0.4000	12.5500	0.2015	0.1000	1.1480
4.0000	0.2000	10.0300	0.1593	0.1000	1.1950
2.0000	1.0000	13.3900	0.2180	0.1000	0.7768
2.0000	0.8000	12.4600	0.2022	0.1000	0.8284
2.0000	0.6000	11.3500	0.1834	0.1000	0.8695
2.0000	0.4000	9.9620	0.1600	0.1000	0.9112
2.0000	0.2000	7.9420	0.1260	0.1000	0.9507

CASE 1 ECHO-(FRITZ/CONMIN)

-NX (KIPS/IN)	PHI	WEIGHT (LBS)	T1 (IN)	T2 (IN)	H (IN)
16.0000	1.0000	27.0500	0.4340	0.1535	1.6430
16.0000	0.8000	25.0200	0.4035	0.1327	1.6430
16.0000	0.6000	22.8000	0.3669	0.1282	1.6300
16.0000	0.4000	19.9900	0.3193	0.1193	1.7490
16.0000	0.2000	15.9500	0.2526	0.1031	1.9190
8.0000	1.0000	21.3500	0.3452	0.1091	1.4630
8.0000	0.8000	19.7700	0.3211	0.0941	1.3520
8.0000	0.6000	18.0400	0.2919	0.0906	1.4420
8.0000	0.4000	15.7700	0.2541	0.0849	1.5460
8.0000	0.2000	12.5700	0.2012	0.0733	1.6940
4.0000	1.0000	16.8700	0.2746	0.0768	1.2920
4.0000	0.8000	15.6500	0.2555	0.0666	1.1980
4.0000	0.6000	14.2600	0.2322	0.0645	1.2760
4.0000	0.4000	12.4700	0.2024	0.0600	1.3700
4.0000	0.2000	9.9170	0.1601	0.0519	1.5000
2.0000	1.0000	13.3800	0.2184	0.0628	1.0900
2.0000	0.8000	12.3800	0.2032	0.0458	1.0280
2.0000	0.6000	11.2700	0.1846	0.0440	1.0920
2.0000	0.4000	9.8560	0.1610	0.0417	1.1600
2.0000	0.2000	7.8290	0.1272	0.0400	1.2720

Table 1A: Case 1 Blade Stiffened Flat Panel-Optimization with PANDA; ECHO-(FRITZ/CONMIN)

CASE 2 PANDA

-NX (KIPS/IN)	PHI	WEIGHT (LBS)	T1 (IN)	T2 (IN)	H (IN)
16.0000	1.0000	18.1600	0.2763	0.1505	1.3110
16.0000	0.8000	16.8000	0.2555	0.1435	1.3470
16.0000	0.6000	15.3900	0.2317	0.1340	1.3920
16.0000	0.4000	13.5300	0.2019	0.1219	1.4520
16.0000	0.2000	10.8400	0.1590	0.1030	1.5500
8.0000	1.0000	14.2200	0.2206	0.1069	1.1610
8.0000	0.8000	13.2200	0.2041	0.1020	1.1930
8.0000	0.6000	12.0700	0.1850	0.1000	1.2140
8.0000	0.4000	10.6400	0.1610	0.1000	1.2300
8.0000	0.2000	8.5920	0.1266	0.1000	1.2470
4.0000	1.0000	11.2500	0.1750	0.1000	0.9420
4.0000	0.8000	10.4800	0.1620	0.1000	0.9530
4.0000	0.6000	9.5770	0.1460	0.1000	0.9630
4.0000	0.4000	8.4400	0.1277	0.1000	0.9740
4.0000	0.2000	6.8100	0.1005	0.1000	0.9897
2.0000	1.0000	8.9000	0.1384	0.1000	0.7480
2.0000	0.8000	8.3100	0.1285	0.1000	0.7557
2.0000	0.6000	7.6040	0.1165	0.1000	0.7649
2.0000	0.4000	6.6990	0.1013	0.1000	0.7737
2.0000	0.2000	5.4120	0.0797	0.1000	0.7854

CASE 2 ECHO-(FRITZ/CONMIN)

-NX (KIPS/IN)	PHI	WEIGHT (LBS)	T1 (IN)	T2 (IN)	H (IN)
16.0000	1.0000	18.3400	0.2742	0.1639	1.4410
16.0000	0.8000	16.9600	0.2552	0.1478	1.3920
16.0000	0.6000	15.4700	0.2312	0.1383	1.4400
16.0000	0.4000	13.6100	0.2015	0.1260	1.5060
16.0000	0.2000	10.9100	0.1585	0.1065	1.6210
8.0000	1.0000	14.3200	0.2192	0.1155	1.2590
8.0000	0.8000	13.2500	0.2039	0.1043	1.2230
8.0000	0.6000	12.0800	0.1849	0.0978	1.2650
8.0000	0.4000	10.6100	0.1611	0.0827	1.3220
8.0000	0.2000	8.4860	0.1271	0.0755	1.4210
4.0000	1.0000	11.2200	0.1751	0.0811	1.1040
4.0000	0.8000	10.4000	0.1628	0.0736	1.0780
4.0000	0.6000	9.4770	0.1477	0.0689	1.1160
4.0000	0.4000	8.3110	0.1287	0.0629	1.1650
4.0000	0.2000	6.6410	0.1018	0.0532	1.2500
2.0000	1.0000	8.8270	0.1397	0.0571	0.9202
2.0000	0.8000	8.1860	0.1298	0.0521	0.9524
2.0000	0.6000	7.4440	0.1[illegible]40	0.0477	0.9583
2.0000	0.4000	6.5160	0.1028	0.0434	0.9962
2.0000	0.2000	5.2140	0.0814	0.0400	1.0320

Table 2A: Case 2 Blade Stiffened Flat Panel-Optimization with PANDA; ECHO

CASE 3 PANDA

-NX (KIPS/IN)	PHI	WEIGHT (LBS)	T1 (IN)	T2 (IN)	H (IN)
8.0000	1.0000	67.2100	0.2104	0.2004	2.6040
8.0000	0.8000	62.8600	0.1940	0.1890	2.6620
8.0000	0.6000	57.5900	0.1790	0.1750	2.7400
8.0000	0.4000	51.0200	0.1530	0.1570	2.8600
8.0000	0.2000	41.1500	0.1197	0.1299	3.0700
6.0000	1.0000	60.1700	0.1930	0.1750	2.4600
6.0000	0.8000	56.1500	0.1790	0.1650	2.5100
6.0000	0.6000	51.4600	0.1616	0.1530	2.5900
6.0000	0.4000	45.5000	0.1401	0.1380	2.6960
6.0000	0.2000	36.9600	0.1099	0.1140	2.9000
4.0000	1.0000	51.4000	0.1700	0.1450	2.2700
4.0000	0.8000	47.9700	0.1580	0.1360	2.3200
4.0000	0.6000	43.9400	0.1430	0.1270	2.3900
4.0000	0.4000	38.8100	0.1240	0.1140	2.4900
4.0000	0.2000	31.6700	0.0969	0.1000	2.6300
2.0000	1.0000	39.5700	0.1371	0.1044	1.9900
2.0000	0.8000	36.9400	0.1270	0.1000	2.0200
2.0000	0.6000	33.8600	0.1140	0.1000	2.0400
2.0000	0.4000	29.9700	0.0970	0.1000	2.0600
2.0000	0.2000	25.1200	0.0769	0.1000	2.0900

CASE 3 ECHO-(FRITZ/CONMIN)

-NX (KIPS/IN)	PHI	WEIGHT (LBS)	T1 (IN)	T2 (IN)	H (IN)
8.0000	1.0000	70.8100	0.2050	0.2213	3.0500
8.0000	0.8000	64.5400	0.1920	0.1991	2.8990
8.0000	0.6000	59.5000	0.1734	0.1859	3.0060
8.0000	0.4000	52.9700	0.1501	0.1684	3.1420
8.0000	0.2000	43.2100	0.1174	0.1389	3.3840
6.0000	1.0000	62.9300	0.1883	0.1934	2.8670
6.0000	0.8000	57.5100	0.1763	0.1745	2.7220
6.0000	0.6000	52.8200	0.1592	0.1627	2.8080
6.0000	0.4000	46.8500	0.1384	0.1484	2.9450
6.0000	0.2000	38.2800	0.1082	0.1211	3.1770
4.0000	1.0000	53.4800	0.1668	0.1605	2.6200
4.0000	0.8000	49.0000	0.1561	0.1447	2.4940
4.0000	0.6000	44.9300	0.1410	0.1350	2.5700
4.0000	0.4000	39.8500	0.1223	0.1217	2.6980
4.0000	0.2000	32.3500	0.0960	0.1001	2.9070
2.0000	1.0000	40.7400	0.1351	0.1152	2.2540
2.0000	0.8000	37.4300	0.1262	0.1034	2.1590
2.0000	0.6000	34.2400	0.1142	0.0959	2.2270
2.0000	0.4000	30.2500	0.0992	0.0866	2.3240
2.0000	0.2000	24.5500	0.0782	0.0723	2.5010

Table 3A: Case 3 Blade Stiffened Flat Panel-Optimization with PANDA; ECHO

CASE 4B BLADE STIFFENED CURVED PANEL-OPTIMIZED WITH ECHO-(FRITZ/CONMIN)

NXY (KIPS/IN)	-NX (KIPS/IN)	PHI	WEIGHT (LBS)	T1 (MILS)	T2 (MILS)	H (IN)
0.0000	3.0000	1.0000	6.6140	8.6790	6.4780	1.4570
0.0000	3.0000	0.8000	6.2210	7.9470	6.4530	1.5780
0.0000	3.0000	0.6000	5.7200	7.1190	6.1780	1.6980
0.0000	3.0000	0.4000	5.0430	6.0700	5.7340	1.8290
0.0000	3.0000	0.2500	4.2890	5.0000	5.0000	1.9780
1.0000	3.0000	1.0000	6.6830	8.8220	6.4210	1.4360
1.0000	3.0000	0.8000	6.2810	8.0810	6.3440	1.5650
1.0000	3.0000	0.6000	5.7830	7.2440	6.1140	1.6800
1.0000	3.0000	0.4000	5.1130	6.1980	5.6770	1.8260
1.0000	3.0000	0.2300	4.2900	5.0000	5.0000	1.9800

CASE 4B BLADE STIFFENED CURVED PANEL-OPTIMIZED WITH ECHO-(FRITZ/CONMIN)

-NX (KIPS/IN)	PHI	WEIGHT (LBS)	T1 (MILS)	T2 (MILS)	H (IN)
8.0000	1.0000	9.8520	11.8000	10.9400	1.9030
8.0000	0.8000	9.2330	10.8600	10.4400	1.9850
8.0000	0.6000	8.4970	9.7560	9.8160	2.0880
8.0000	0.4000	7.5430	8.3720	8.9510	2.2260
8.0000	0.2000	6.1580	6.4610	7.5440	2.4530
6.0000	1.0000	8.6800	10.8400	9.1920	1.7060
6.0000	0.8000	8.1630	9.9640	8.9110	1.8100
6.0000	0.6000	7.5420	8.9170	8.5620	1.9430
6.0000	0.4000	6.7060	7.6640	7.8310	2.0920
6.0000	0.2000	5.4090	5.8380	6.6430	2.3000
4.0000	1.0000	7.3950	9.5330	7.4800	1.5480
4.0000	0.8000	6.9640	8.7400	7.3740	1.6720
4.0000	0.6000	6.4110	7.8230	7.0700	1.7960
4.0000	0.4000	5.6730	6.6880	6.5290	1.9350
4.0000	0.2000	4.5520	5.0830	5.5600	2.1290
3.0000	1.0000	6.6150	8.6790	6.4850	1.4570
3.0000	0.8000	6.2200	7.9480	6.4300	1.5800
3.0000	0.6000	5.7200	7.1190	6.1780	1.6980
3.0000	0.4000	5.0430	6.0700	5.7340	1.8290
3.0000	0.2450	4.2880	5.0000	5.0000	1.9780

CASE 4J J-STIFFENED CURVED PANEL-OPTIMIZED WITH ECHO-(FRITZ/CONMIN)

NXY (KIPS/IN)	-NX (KIPS/IN)	PHI	WEIGHT (LBS)	T1 (MILS)	T2 (MILS)	H (IN)
0.0000	3.0000	1.0000	6.4800	8.5830	5.0000	0.9679
0.0000	3.0000	0.8000	6.0760	7.8530	5.0000	1.0370
0.0000	3.0000	0.6000	5.5850	6.9980	5.0000	1.0990
0.0000	3.0000	0.4000	4.9500	5.9200	5.0000	1.1610
0.0000	3.0000	0.2700	4.3920	5.0000	5.0000	1.1970
1.0000	3.0000	1.0000	6.5530	8.7320	5.0000	0.9443
1.0000	3.0000	0.8000	6.1540	7.9970	5.0000	1.0210
1.0000	3.0000	0.6000	5.6680	7.1340	5.0000	1.0930
1.0000	3.0000	0.4000	5.0340	6.0650	5.0000	1.1510
1.0000	3.0000	0.2500	4.3920	5.0000	5.0000	1.1960

Table 4A: Blade and J Stiffened Correct Panel-Optimization with ECHO(FRITZ/CONMIN)

TABLE 5A: Failure Loads for Imperfect Blade Stiffened Curved Panel (CASE 4B)

PHI=.2   N=4000

INPUT DATA VALUES

.379200+04
.375000+04
.375000+04
.360400+04
.300000+04
.379200+04
.375000+04
.294200+04
.375000+04
.379200+04

THE AVERAGE OF THE DATA IS .359220+04
THE STANDARD DEVIATION ESTIMATE IS .332159+03

PROBABILITY	HIGH	LOW
.900000+00	.405159+04	.313281+04
.990000+00	.452937+04	.265503+04

PHI=.2   N=3000

INPUT DATA VALUES

.260400+04
.327000+04
.325000+04
.260400+04
.327000+04
.289600+04
.324100+04
.327000+04
.381200+04

THE AVERAGE OF THE DATA IS .313522+04
THE STANDARD DEVIATION ESTIMATE IS .380544+03

PROBABILITY	HIGH	LOW
.900000+00	.366677+04	.260367+04
.990000+00	.423745+04	.203299+04

TABLE 5A, continued

PHI = .2 N=8000

INPUT DATA VALUES

.476300+04
.477900+04
.457900+04
.478300+04
.478300+04
.471700+04
.472100+04
.472100+04
.470800+04
.474600+04

THE AVERAGE OF THE DATA IS .473000+04
THE STANDARD DEVIATION ESTIMATE IS .605328+02

PROBABILITY	HIGH	LOW
.900000+00	.481372+04	.464628+04
.990000+00	.490079+04	.455921+04

PHI = .2 N=6000

INPUT DATA VALUES

.437100+04
.439600+04
.440800+04
.441000+04
.434300+04
.437500+04
.441200+04
.412500+04
.416600+04
.418800+04

THE AVERAGE OF THE DATA IS .431940+04
THE STANDARD DEVIATION ESTIMATE IS .113236+03

PROBABILITY	HIGH	LOW
.900000+00	.447601+04	.416279+04
.990000+00	.463889+04	.399991+04

TABLE 5A, continued

PHI=.4 N=4000

INPUT DATA VALUES

.512200+04
.512300+04
.511100+04
.383500+04
.511500+04
.512800+04
.514200+04
.510600+04
.511700+04
.398800+04

THE AVERAGE OF THE DATA IS .487870+04
THE STANDARD DEVIATION ESTIMATE IS .511128+03

PROBABILITY	HIGH	LOW
.900000+00	.558561+04	.417179+04
.990000+00	.632082+04	.343658+04

PHI=.4 N=3000

INPUT DATA VALUES

.333900+04
.329100+04
.334000+04
.330300+04
.330600+04
.323600+04
.325300+04
.422800+04
.328000+04
.326600+04

THE AVERAGE OF THE DATA IS .338420+04
THE STANDARD DEVIATION ESTIMATE IS .298403+03

PROBABILITY	HIGH	LOW
.900000+00	.379690+04	.297150+04
.990000+00	.422612+04	.254228+04

TABLE 5A, continued

PHI = .4 N=8000

INPUT DATA VALUES

.627100+04
.611500+04
.628200+04
.625400+04
.588500+04
.613500+04
.574300+04
.628300+04
.625600+04
.574900+04

THE AVERAGE OF THE DATA IS .609730+04
THE STANDARD DEVIATION ESTIMATE IS .221649+03

PROBABILITY	HIGH	LOW
.900000+00	.640385+04	.579075+04
.990000+00	.672267+04	.547193+04

PHI = .4 N=6000

INPUT DATA VALUES

.581100+04
.580100+04
.514100+04
.581300+04
.578100+04
.508900+04
.579400+04
.580400+04
.578700+04
.579600+04

THE AVERAGE OF THE DATA IS .566170+04
THE STANDARD DEVIATION ESTIMATE IS .288565+03

PROBABILITY	HIGH	LOW
.900000+00	.606079+04	.526261+04
.990000+00	.647587+04	.484753+04

TALBE 5A, continued

PHI = .6   N=4000

INPUT DATA VALUES

.603800+04
.603700+04
.603600+04
.423200+04
.603100+04
.431600+04
.428800+04
.603400+04
.603700+04
.603800+04

THE AVERAGE OF THE DATA IS .550870+04
THE STANDARD DEVIATION ESTIMATE IS .849046+03

PROBABILITY	HIGH	LOW
.900000+00	.668295+04	.433445+04
.990000+00	.790423+04	.311317+04

PHI = .6   N=3000

INPUT DATA VALUES

.552700+04
.553200+04
.365500+04
.365800+04
.554900+04
.371300+04
.372600+04
.553700+04
.554100+04
.553200+04

THE AVERAGE OF THE DATA IS .479700+04
THE STANDARD DEVIATION ESTIMATE IS .954729+03

PROBABILITY	HIGH	LOW
.900000+00	.611742+04	.347658+04
.990000+00	.749071+04	.210329+04

TABLE 5A, continued

PHI=.6 N=8000

INPUT DATA VALUES

.661800+04
.737100+04
.740300+04
.661800+04
.737700+04
.740400+04
.662000+04
.643100+04
.644200+04
.765200+04

THE AVERAGE OF THE DATA IS .699360+04
THE STANDARD DEVIATION ESTIMATE IS .483214+03

PROBABILITY	HIGH	LOW
900000+00	.766190+04	.632530+04
.990000+00	.835696+04	.563024+04

PHI= 6 N=6000

INPUT DATA VALUES

.558000+04
.680900+04
.558800+04
.554600+04
.557500+04
.556000+04
.554500+04
.680700+04
.556500+04
.554900+04

THE AVERAGE OF THE DATA IS .581240+04
THE STANDARD DEVIATION ESTIMATE IS .524927+03

PROBABILITY	HIGH	LOW
.900000+00	653839+04	.508641+04
990000+00	.729345+04	.433135+04

TABLE 5A, continued

PHI=.8 N=4000

INPUT DATA VALUES

.679600+04
.459500+04
.460200+04
.454000+04
.678100+04
.680500+04
.452600+04
.680600+04
.679700+04
.678300+04

THE AVERAGE OF THE DATA IS .590310+04
THE STANDARD DEVIATION ESTIMATE IS .115125+04

PROBABILITY	HIGH	LOW
.900000+00	.749531+04	.431089+04
.990000+00	.915127+04	.265493+04

PHI=.8 N=3000

INPUT DATA VALUES

.621700+04
.395300+04
.395300+04
.395000+04
.394300+04
.623300+04
.584500+04
.497000+04
.622400+04
.583100+04

THE AVERAGE OF THE DATA IS .511190+04
THE STANDARD DEVIATION ESTIMATE IS .106416+04

PROBABILITY	HIGH	LOW
.900000+00	.658367+04	.364013+04
.990000+00	.811437+04	.210943+04

TABLE 5A, continued

PHI=.8 N=8000

INPUT DATA VALUES

.828000+04
.828400+04
.826000+04
.822300+04
.828300+04
.825500+04
.825100+04
.827100+04
.720300+04
.838900+04

THE AVERAGE OF THE DATA IS .816990+04
THE STANDARD DEVIATION ESTIMATE IS .342510+03

PROBABILITY	HIGH	LOW
.900000+00	.864360+04	.769620+04
.990000+00	.913627+04	.720353+04

PHI=.8 N=6000

INPUT DATA VALUES

.580000+04
.583400+04
.584400+04
.609700+04
.579900+04
.766600+04
.584300+04
.584600+04
.574100+04
.582100+04

THE AVERAGE OF THE DATA IS .602910+04
THE STANDARD DEVIATION ESTIMATE IS .582740+03

PROBABILITY	HIGH	LOW
.900000+00	.683505+04	.522315+04
.990000+00	.767327+04	.438493+04

TABLE 5A, continued

PHI=1. N=4000

INPUT DATA VALUES

.481200+04
.744200+04
.745000+04
.747700+04
.493000+04
.746600+04
.488000+04
.746000+04
.747100+04
.497300+04

THE AVERAGE OF THE DATA IS .643610+04
THE STANDARD DEVIATION ESTIMATE IS .132378+04

PROBABILITY	HIGH	LOW
.900000+00	.826693+04	.460527+04
.990000+00	.101711+05	.270114+04

PHI=1. N=3000

INPUT DATA VALUES

.409300+04
.414800+04
.684200+04
.683300+04
.684700+04
.683500+04
.428200+04
.683700+04
.685100+04
.684300+04

THE AVERAGE OF THE DATA IS .604110+04
THE STANDARD DEVIATION ESTIMATE IS .128902+04

PROBABILITY	HIGH	LOW
.900000+00	.782385+04	.425835+04
.990000+00	.967798+04	.240422+04

TABLE 5A, continued

PHI=1.   N=8000

INPUT DATA VALUES

.752200+04
.898900+04
.779500+04
.897200+04
.899600+04
.901000+04
.902100+04
.898600+04
.779300+04
.898400+04

THE AVERAGE OF THE DATA IS .860680+04
THE STANDARD DEVIATION ESTIMATE IS .627979+03

PROBABILITY	HIGH	LOW
.900000+00	.947531+04	.773829+04
.990000+00	.103786+05	.683499+04

PHI=1.   N=6000

INPUT DATA VALUES

.839000+04
.619800+04
.621600+04
.612200+04
.612400+04
.838800+04
.614000+04
.615700+04
.615100+04
.838700+04

THE AVERAGE OF THE DATA IS .682730+04
THE STANDARD DEVIATION ESTIMATE IS .107762+04

PROBABILITY	HIGH	LOW
.900000+00	.831768+04	.533692+04
.990000+00	.986773+04	.378687+04

CASE 1 BLADE STIFFENED PANEL PANDA

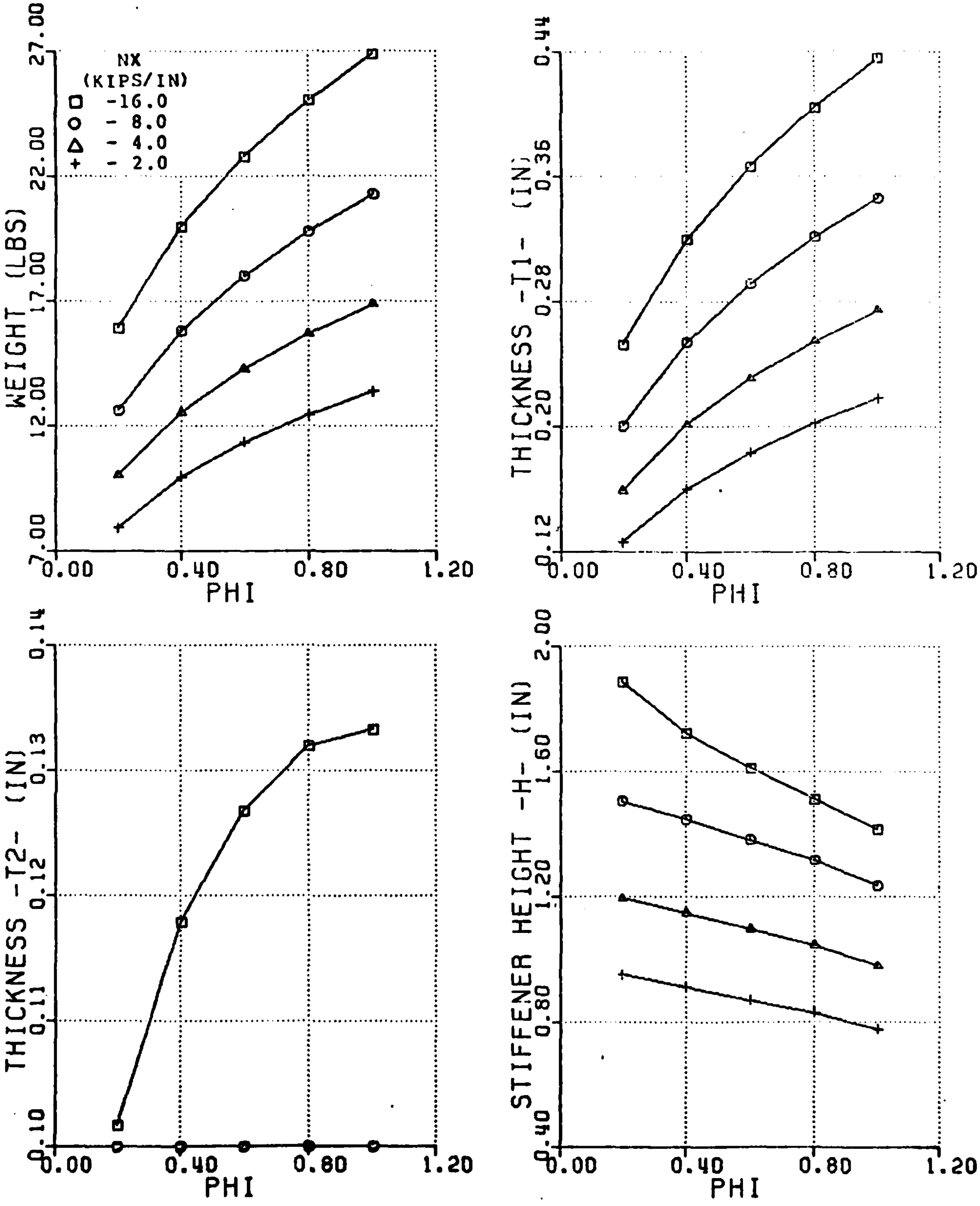

Figure 1A Case 1 Blade Stiffened Flat Panel-Optimization With PANDA

CASE 1 BLADE STIFFENED PANEL ECHO-FRITZ/CONMIN

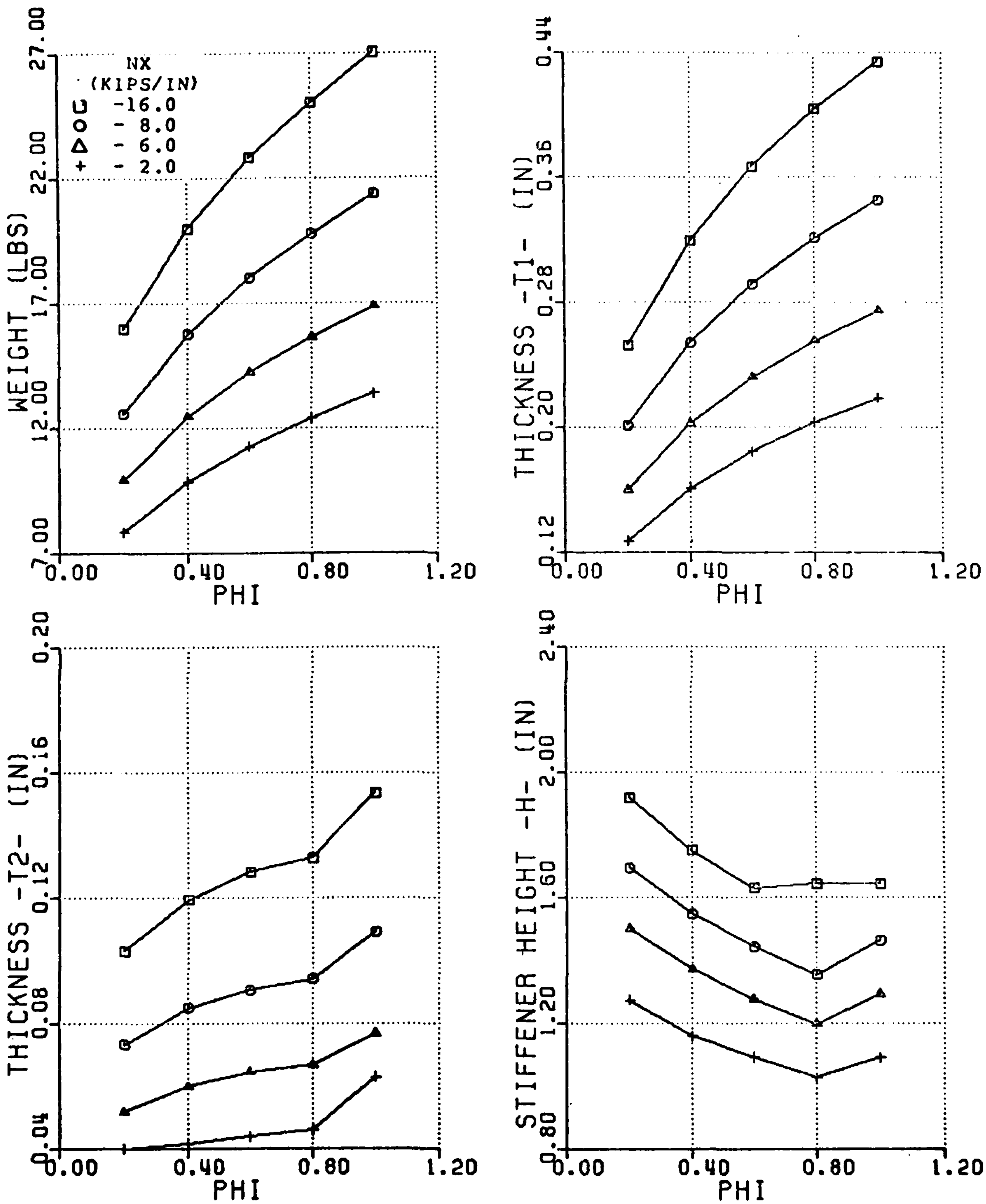

Figure 2A Case 1 Blade Stiffened Flat Panel-Optimization With ECHO-(FRITZ/CONMIN)

CASE 2 BLADE STIFFENED PANEL PANDA

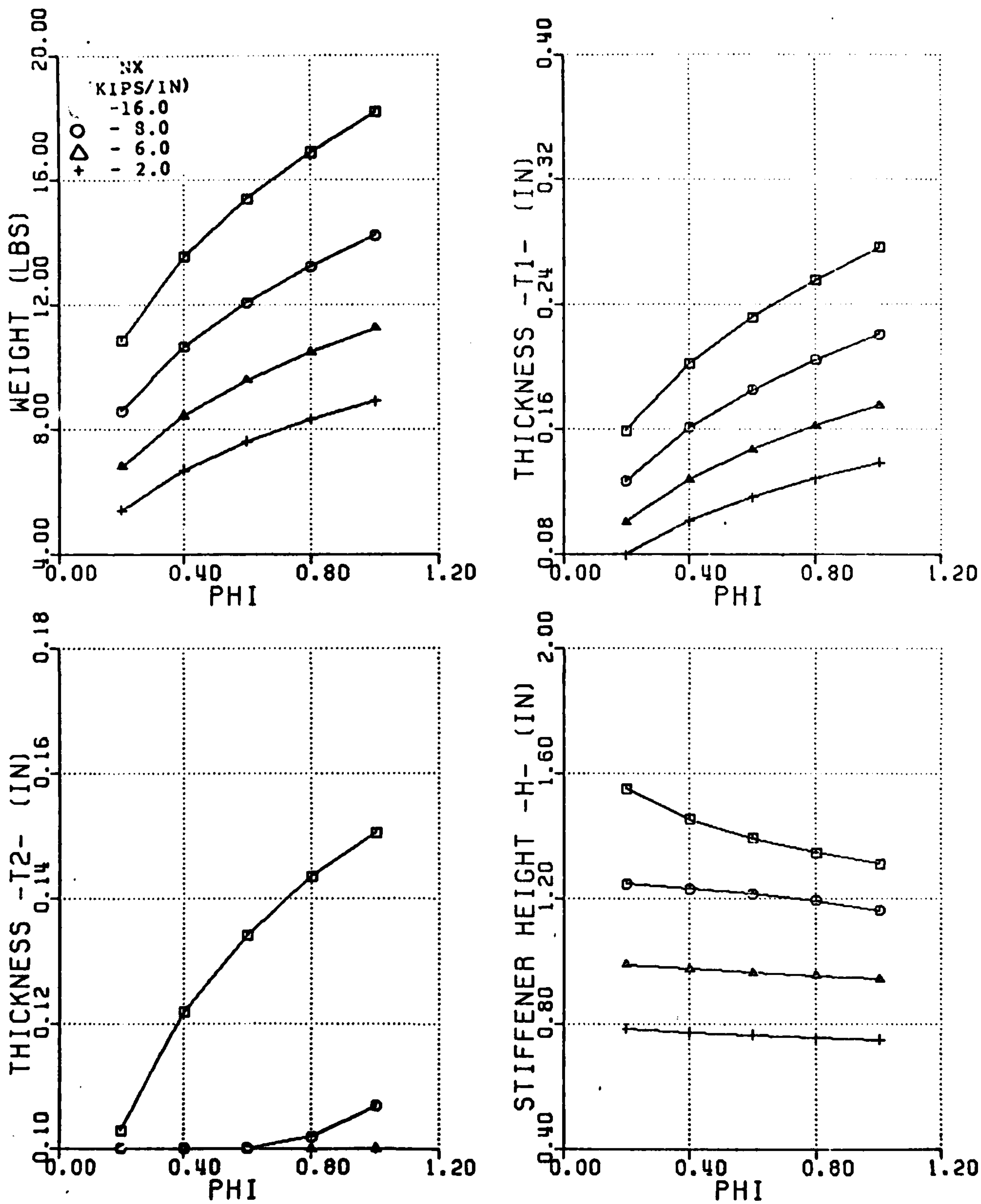

Figure 3A Case 2 Blade Stiffened Flat Panel-Optimization With PANDA

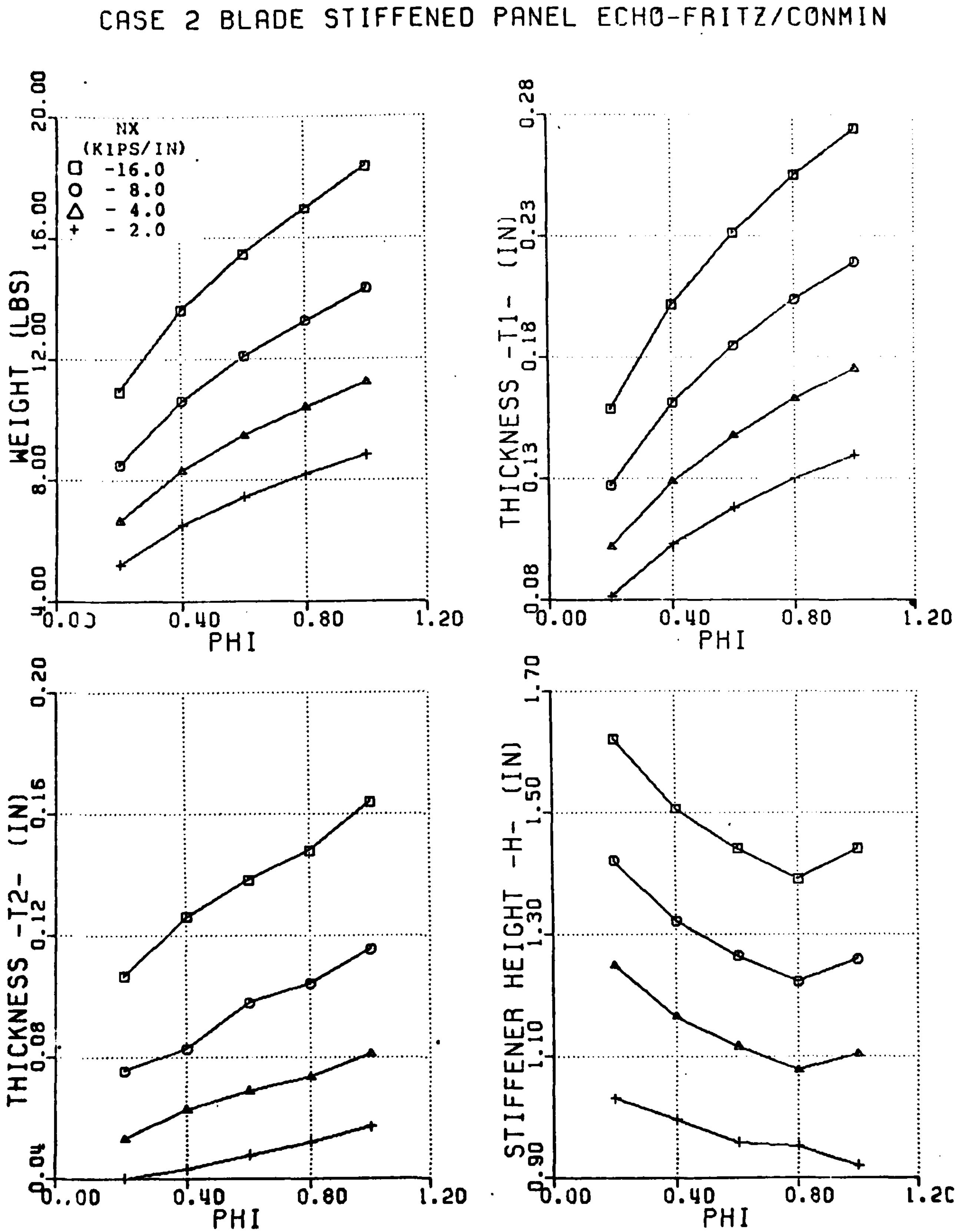

Figure 4A Case 2 Blade Stiffened Flat Panel-Optimization With ECHO-(FRITZ/CONMIN)

CASE 3 BLADE STIFFENED PANEL PANDA

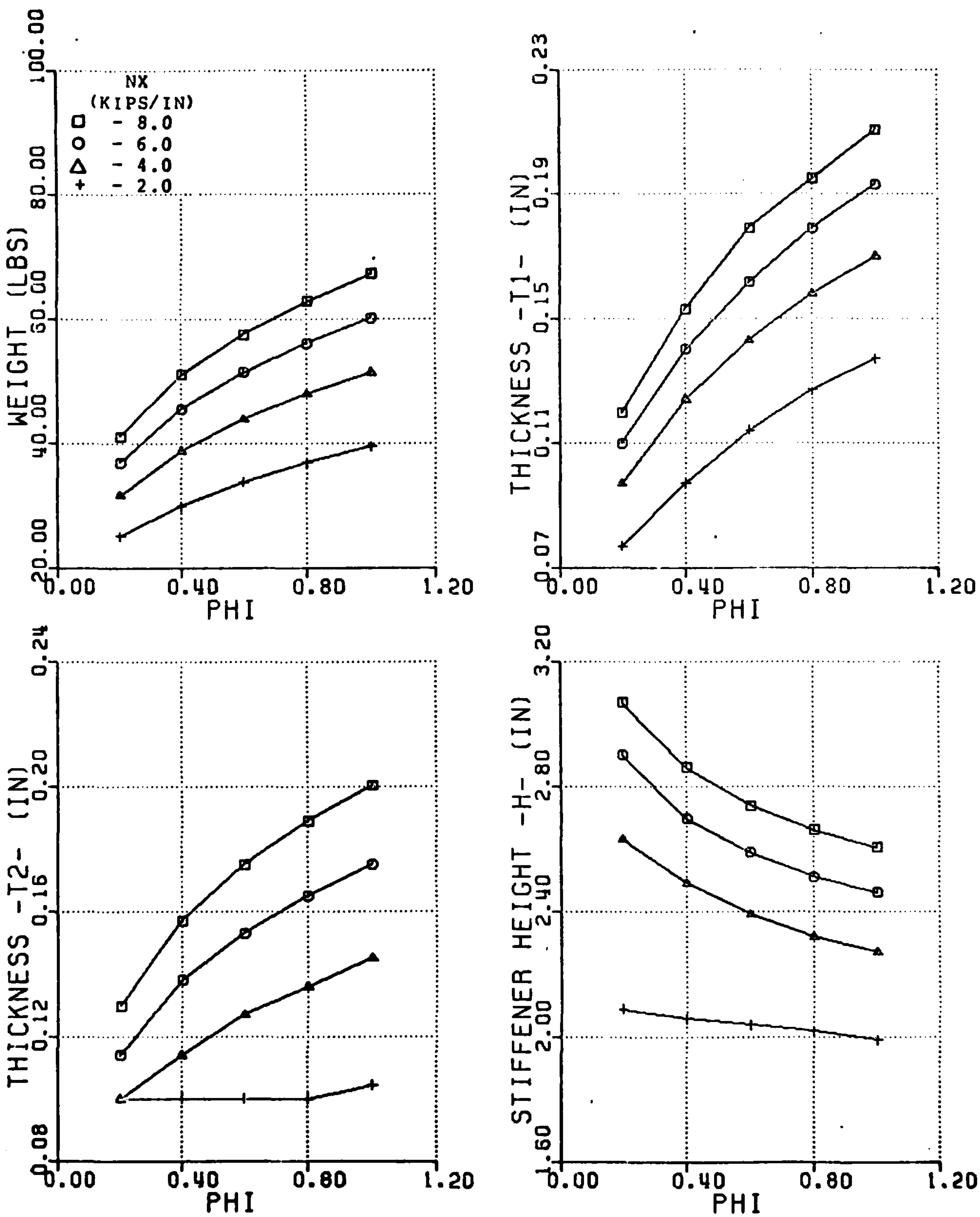

Figure 5A Case 3 Blade Stiffened Flat Panel-Optimization With PANDA

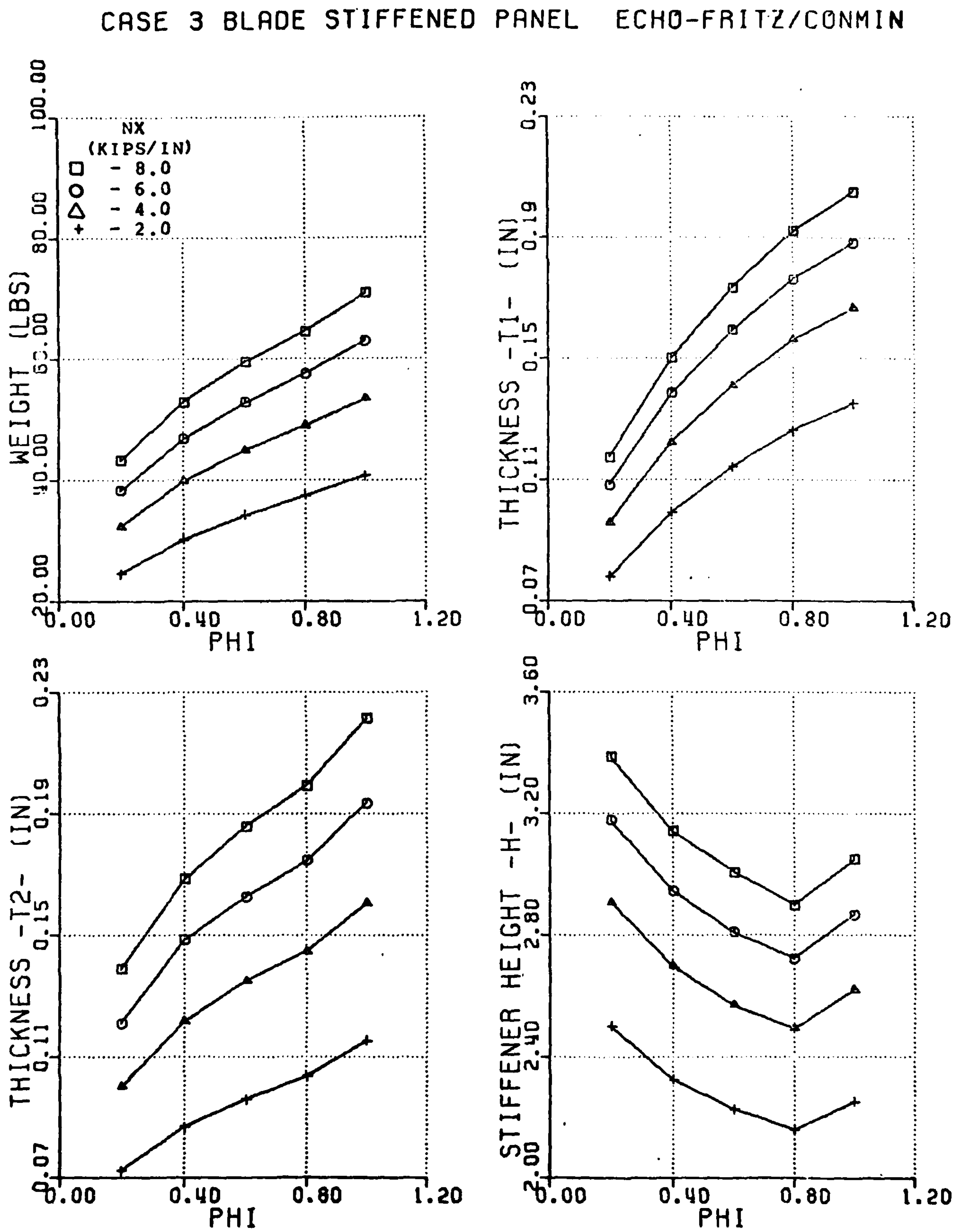

Figure 6A Case 3 Blade Stiffened Flat Panel-Optimization With ECHO-(FRITZ/CONMIN)

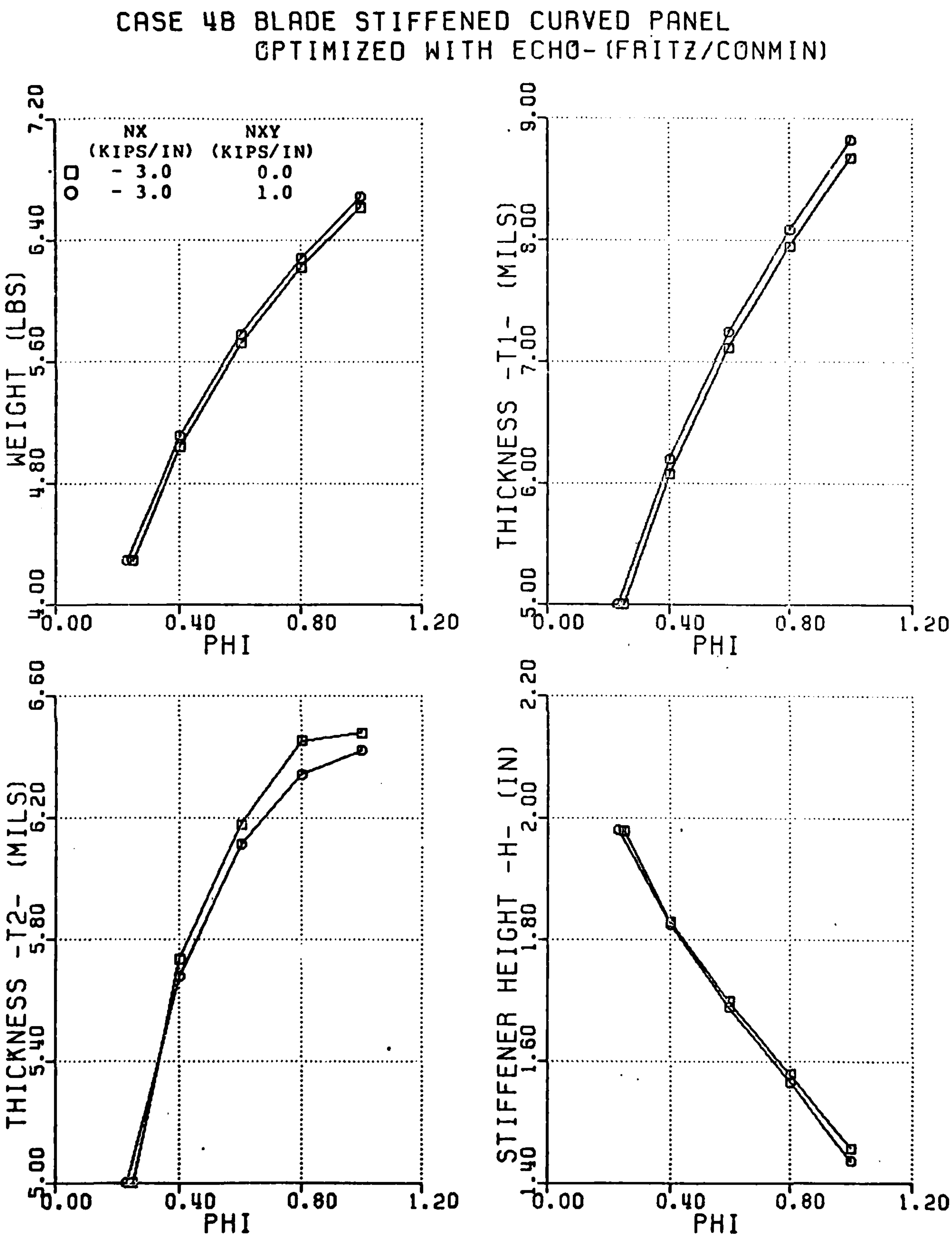

Figure 7A Case 4B Blade Stiffened Curved Panel-Optimization With ECHO-(FRITZ/CONMIN)

CASE 4B BLADE STIFFENED CURVED PANEL
ECHO -FRITZ/CONMIN

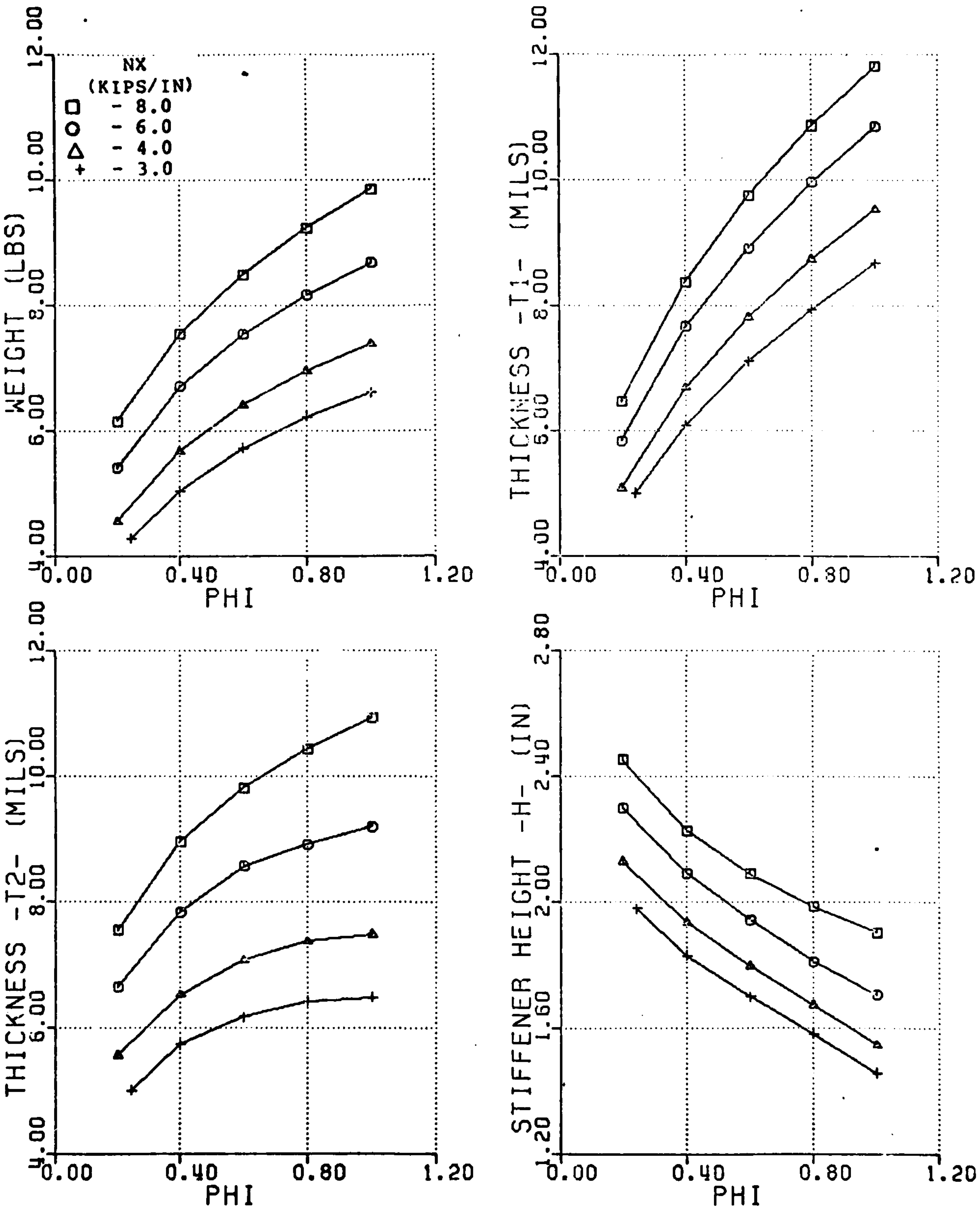

Figure 8A Case 4B Blade Stiffened Curved Panel-Optimization With ECHO-(FRITZ/CONMIN)

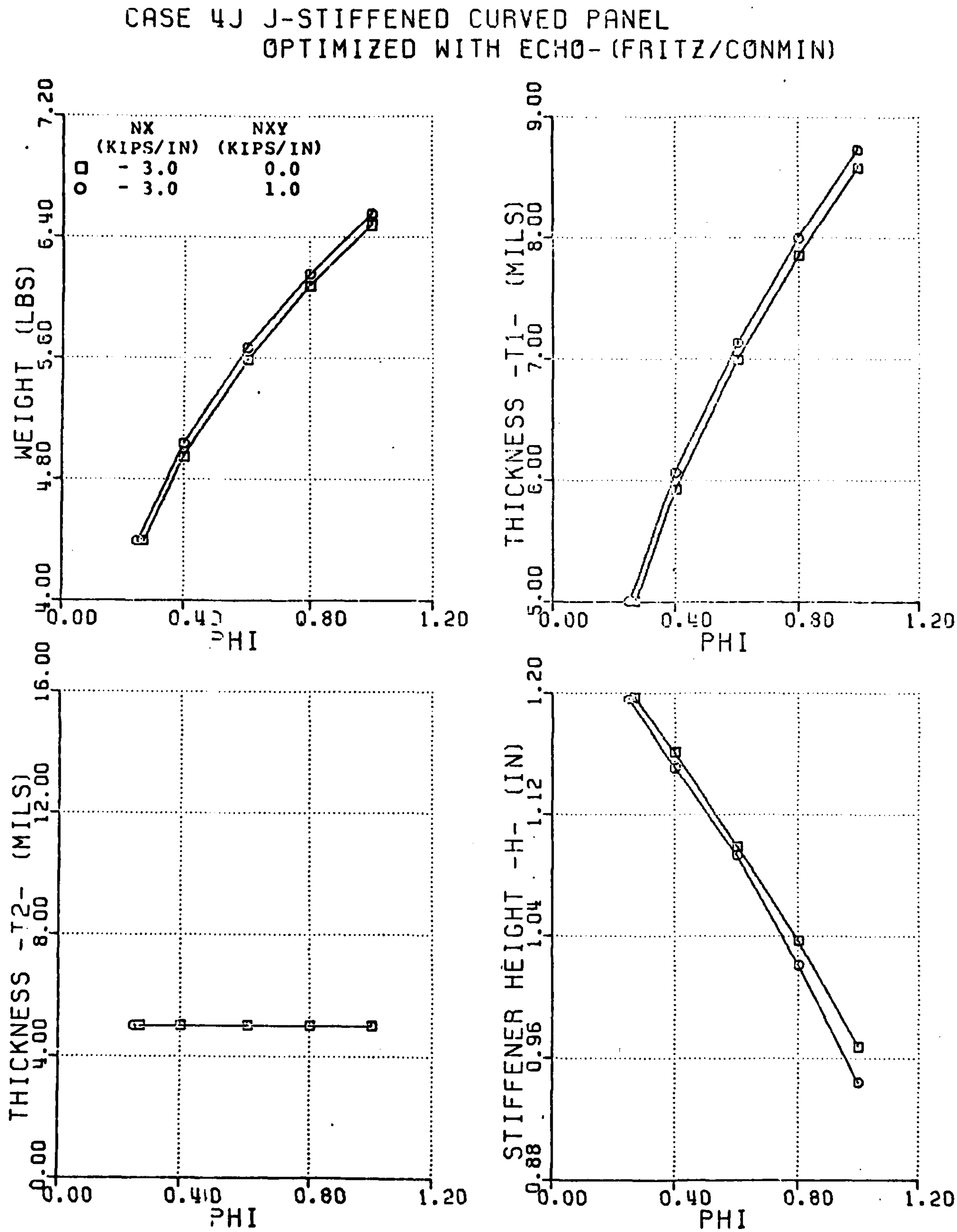

Figure 9A Case 4J J-Stiffened Curved Panel-Optimization With ECHO-(FRITZ/CONMIN)

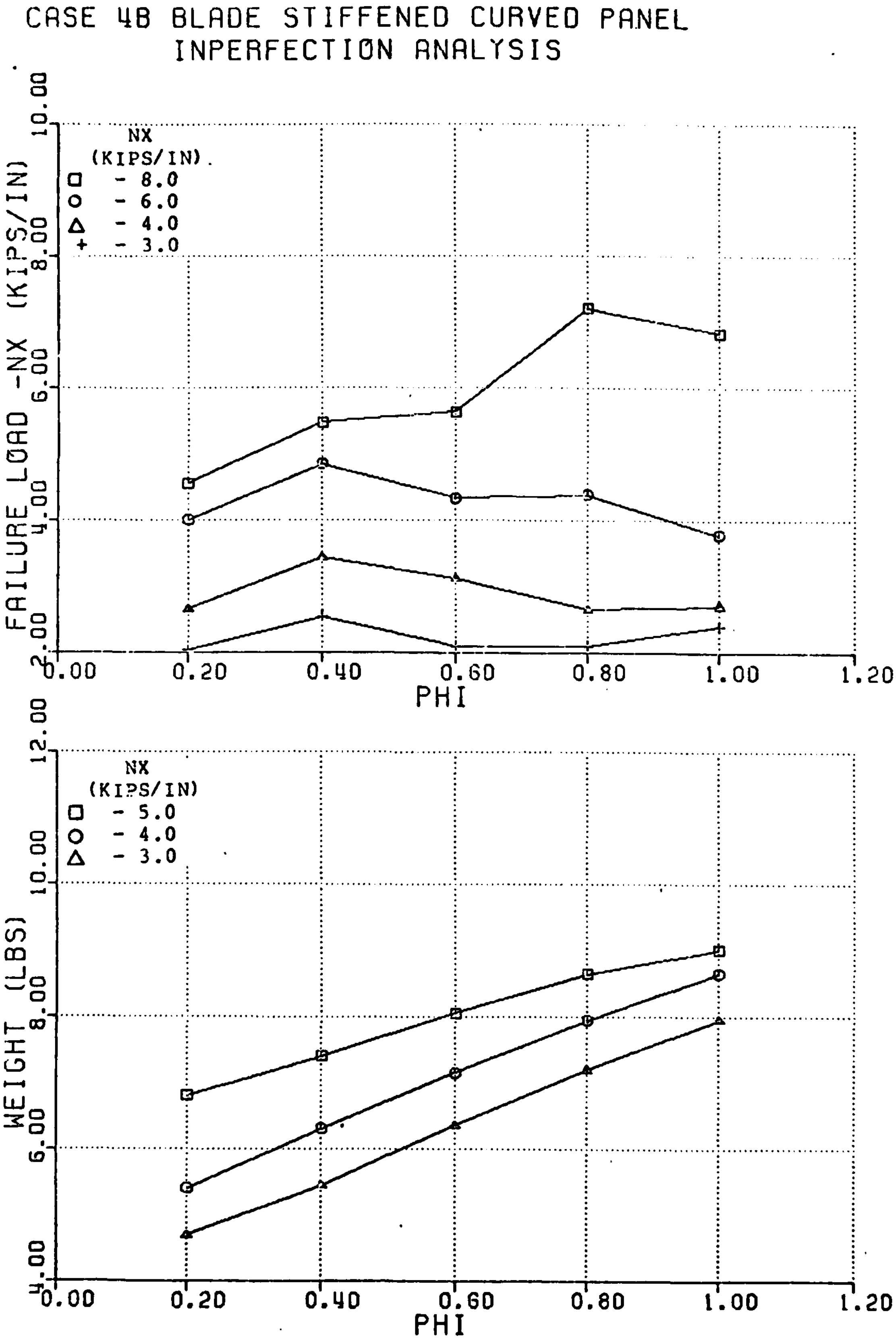

Figure 10A Case 4B Blade Stiffened Curved Panel
Imperfection Analysis With ECHO-(FRITZ)

8

DTIC